

Metal-Organic Fireworks! Coordination polymers as integrated structural scaffolds for pyrotechnic materials

Lisa H. Blair, Simon J. Coles, Ayhan Colakel, Ian Sinclair, Ranko Vrcelj*

Supporting Information

1. General Methods

The oxidisers (calcium nitrate, strontium nitrate, barium nitrate, rubidium nitrate, and cesium nitrate) were obtained from Wallop Defence Systems Limited. Sodium nitrate and potassium nitrate were purchased from Sigma-Aldrich. Terephthalic acid (BDC) was purchased from Alfa Aesar and tetrafluoroterephthalic acid (fBDC) was purchased from Fluorochem. The other reagents used in the following experiments were of analytical grade or better unless otherwise stated. These materials were used without purification. The structural characterisation was carried out using single crystal and powder x-ray diffraction. The thermal analysis of each MOF described below was carried out using a Mettler-Toledo differential scanning calorimeter instrument, model DSC821e, equipped with a liquid nitrogen low temperature attachment and a TSO801RO Universal sample robot (heating rate: 10°Cmin⁻¹; the flow rate of nitrogen gas: 40ml/min; the sample size: 4 – 10mg in 40µl aluminium dishes).

2. Synthetic Procedures

The initial synthetic procedure was adapted from a MOF5 synthesis ^[1]. 4mmol metal nitrate and 2mmol 1,2-BDC/1,3-BDC/1,4-BDC/1,2-fBDC/1,3-fBDC/1,4-fBDC was added to 40 ml DMF and stirred at room temperature. (Sr(NO₃)₂ and Ba(NO₃)₂ were stirred overnight before the addition of the diacid). Once a colourless solution was observed 2.2ml TEA(deprotonating agent) was added dropwise. After stirring for 30-45 minutes a white precipitate was collected using a sinter funnel. The product was immersed in chloroform for 24 hours to exchange DMF solution.

The second synthetic procedure used in this work was adapted from another synthesis used by W. Clegg and L. Russo to investigate alkali metal complexes of isophthalic acid. ^[2] 0.5mmol metal nitrate was added to a conical flask containing methanol (Na, Ca nitrates = 10ml; K, Ru, Sr nitrates = 20ml; Cs, Ba nitrates = 30ml). The solutions were allowed to stir for 2 hours before the addition of 0.5mmol diacid. After stirring for an additional 1 hour, 1ml of pyridine (deprotonating agent) was added dropwise and allowed to stir for 3 hours before being distributed into both glass vials and petri dishes.

(**1** = 1,4BDC; **2** = 1,3-BDC; **3** = 1,2-BDC; **4** = 1,4-fBDC; **5** = 1,3-fBDC; **6** = 1,2-fBDC)

• crystal structure obtained

K1_1 - This complex was obtained following method 1 using KNO₃ (4 mmol, 0.404 g) and 1,4-BDC (2 mmol, 0.332g).

K1_2 - This complex was obtained following method 2 using KNO₃ (0.5 mmol, 0.051g) and 1,4-BDC (0.5 mmol, 0.083g).

K2_1 - This complex was obtained following method 1 using KNO₃ (4 mmol, 0.404 g) and 1,3-BDC (2 mmol, 0.332g).

K2_2 - This complex was obtained following method 2 using KNO₃ (0.5 mmol, 0.051g) and 1,3-BDC (0.5 mmol, 0.083g).

K3_1 - This complex was obtained following method 1 using KNO₃ (4 mmol, 0.404 g) and 1,2-BDC (2 mmol, 0.332g).

K3_2 - This complex was obtained following method 2 using KNO₃ (0.5 mmol, 0.051g) and 1,2-BDC (0.5 mmol, 0.083g).

***K4_2** - This complex was obtained following method 2 using KNO₃ (0.5 mmol, 0.051g) and 1,4-fBDC (0.5 mmol, 0.119g).

K6_1 - This complex was obtained following method 1 using KNO₃ (4 mmol, 0.404 g) and 1,2-fBDC (2 mmol, 0.476g).

Rb1_1 - This complex was obtained following method 1 using RbNO₃ (4 mmol, 0.590g) and 1,4-BDC (2 mmol, 0.332g).

Rb1_2 - This complex was obtained following method 2 using RbNO_3 (0.5 mmol, 0.074g) and 1,4-BDC (0.5 mmol, 0.083g).

***Rb4_2** - This complex was obtained following method 2 using RbNO_3 (0.5mmol, 0.074g) and 1,4-fBDC (0.5mmol, 0.119g).

Cs1_1 - This complex was obtained following method 1 using CsNO_3 (4 mmol, 0.780g) and 1,4-BDC (2 mmol, 0.332g).

Cs1_2 - This complex was obtained following method 2 using CsNO_3 (0.5 mmol, 0.097g) and 1,4-BDC (0.5 mmol, 0.083g).

***Cs4_2** - This complex was obtained following method 2 using CsNO_3 (0.5 mmol, 0.097g) and 1,4-fBDC (0.5 mmol, 0.119g).

Ca1_1 - This complex was obtained following method 1 using $\text{Ca}(\text{NO}_3)_2 \cdot 4\text{H}_2\text{O}$ (4 mmol, 0.945 g) and 1,4-BDC (2 mmol, 0.332 g).

***Ca1_2** - This complex was obtained following method 2 using $\text{Ca}(\text{NO}_3)_2 \cdot 4\text{H}_2\text{O}$ (0.5mmol, 0.118 g) and 1,4-BDC (0.5 mmol, 0.083g).

Ca2_1 - This complex was obtained following method 1 using $\text{Ca}(\text{NO}_3)_2 \cdot 4\text{H}_2\text{O}$ (4 mmol, 0.945 g) and 1,3-BDC (2 mmol, 0.332 g).

Ca2_2 - This complex was obtained following method 2 using $\text{Ca}(\text{NO}_3)_2 \cdot 4\text{H}_2\text{O}$ (0.5mmol, 0.118 g) and 1,3-BDC (0.5 mmol, 0.083g).

Ca3_2 - This complex was obtained following method 2 using $\text{Ca}(\text{NO}_3)_2 \cdot 4\text{H}_2\text{O}$ (0.5mmol, 0.118 g) and 1,2-BDC (0.5 mmol, 0.083g).

Ca4_1 - This complex was obtained following method 1 using $\text{Ca}(\text{NO}_3)_2 \cdot 4\text{H}_2\text{O}$ (4 mmol, 0.945 g) and 1,4-fBDC (2 mmol, 0.476g).

***Ca4_2** - This complex was obtained following method 2 using $\text{Ca}(\text{NO}_3)_2 \cdot 4\text{H}_2\text{O}$ (0.5mmol, 0.118 g) and 1,4-fBDC (0.5 mmol, 0.119g).

Ca5_1 - This complex was obtained following method 1 using $\text{Ca}(\text{NO}_3)_2 \cdot 4\text{H}_2\text{O}$ (4 mmol, 0.945 g) and 1,3-fBDC (2 mmol, 0.476g).

Ca5_2 - This complex was obtained following method 2 using $\text{Ca}(\text{NO}_3)_2 \cdot 4\text{H}_2\text{O}$ (0.5mmol, 0.118 g) and 1,3-fBDC (0.5 mmol, 0.119g).

Ca6_1 - This complex was obtained following method 1 using $\text{Ca}(\text{NO}_3)_2 \cdot 4\text{H}_2\text{O}$ (4 mmol, 0.945 g) and 1,2-fBDC (2 mmol, 0.476g).

***Ca6_2** - This complex was obtained following method 2 using $\text{Ca}(\text{NO}_3)_2 \cdot 4\text{H}_2\text{O}$ (0.5mmol, 0.118 g) and 1,2-fBDC (0.5 mmol, 0.119g).

***Sr1_1** - This complex was obtained following method 1 using $\text{Sr}(\text{NO}_3)_2$ (4 mmol, 0.847g) and 1,4-BDC (2 mmol, 0.332g).

***Sr1_2** - This complex was obtained following method 2 using $\text{Sr}(\text{NO}_3)_2$ (0.5 mmol, 0.106g) and 1,4-BDC (0.5 mmol, 0.083g).

Sr2_1 - This complex was obtained following method 1 using $\text{Sr}(\text{NO}_3)_2$ (4 mmol, 0.847g) and 1,3-BDC (2 mmol, 0.332g).

Sr2_2 - This complex was obtained following method 2 using $\text{Sr}(\text{NO}_3)_2$ (0.5 mmol, 0.106g) and 1,3-BDC (0.5 mmol, 0.083g).

Sr3_2 - This complex was obtained following method 2 using $\text{Sr}(\text{NO}_3)_2$ (0.5 mmol, 0.106g) and 1,2-BDC (0.5 mmol, 0.083g).

Sr4_1 - This complex was obtained following method 1 using $\text{Sr}(\text{NO}_3)_2$ (4 mmol, 0.847g) and 1,4-fBDC (2 mmol, 0.476g).

***Sr4_2** - This complex was obtained following method 2 using $\text{Sr}(\text{NO}_3)_2$ (0.5 mmol, 0.106g) and 1,4-BDC (0.5 mmol, 0.119g).

***Sr5_1** - This complex was obtained following method 1 using Sr(NO₃)₂. (4 mmol, 0.847 g) and 1,3-fBDC (2 mmol, 0.476g).

***Sr5_2** - This complex was obtained following method 2 using Sr(NO₃)₂. (0.5 mmol, 0.106g) and 1,3-fBDC (0.5 mmol, 0.119g).

***Sr6_1** - This complex was obtained following method 1 using Sr(NO₃)₂. (4 mmol, 0.847 g) and 1,2-fBDC (2 mmol, 0.476g).

***Sr6_2** - This complex was obtained following method 2 using Sr(NO₃)₂. (0.5 mmol, 0.106g) and 1,2-fBDC (0.5 mmol, 0.119g).

Ba1_1 - This complex was obtained following method 1 using Ba(NO₃)₂. (4 mmol, 1.045g) and 1,4-BDC (2 mmol, 0.332g).

***Ba1_2** - This complex was obtained following method 2 using Ba(NO₃)₂. (0.5 mmol, 0.131 g) and 1,4-BDC (0.5 mmol, 0.083g).

Ba2_1 - This complex was obtained following method 1 using Ba(NO₃)₂. (4 mmol, 1.045g) and 1,3-BDC (2 mmol, 0.332g).

Ba2_2 - This complex was obtained following method 2 using Ba(NO₃)₂. (0.5 mmol, 0.131 g) and 1,3-BDC (0.5 mmol, 0.083g).

Ba3_2 - This complex was obtained following method 2 using Ba(NO₃)₂. (0.5 mmol, 0.131 g) and 1,2-BDC (0.5 mmol, 0.083g).

Ba4_1 - This complex was obtained following method 1 using Ba(NO₃)₂. (4 mmol, 1.045g) and 1,4-fBDC (2 mmol, 0.476g).

***Ba4_2** - This complex was obtained following method 2 using Ba(NO₃)₂. (0.5 mmol, 0.131 g) and 1,4-fBDC (0.5 mmol, 0.119g).

Ba5_1 - This complex was obtained following method 1 using Ba(NO₃)₂. (4 mmol, 1.045g) and 1,3-fBDC (2 mmol, 0.476g).

Ba5_2 - This complex was obtained following method 2 using Ba(NO₃)₂. (0.5 mmol, 0.131 g) and 1,3-fBDC (0.5 mmol, 0.119g).

Ba6_1 - This complex was obtained following method 1 using Ba(NO₃)₂. (4 mmol, 1.045g) and 1,2-fBDC (2 mmol, 0.476g).

***Ba6_2** - This complex was obtained following method 2 using Ba(NO₃)₂. (0.5 mmol, 0.131 g) and 1,2-fBDC (0.5 mmol, 0.119g).

The successful syntheses and crystal structure determinations can be summarised in the following table:

	1	2	3	4	5	6
K	MeOH/ DMF x	MeOH/ DMF x	MeOH/ DMF x	MeOH ✓	No product	DMF x
Rb	MeOH/ DMF x	No product	No product	MeOH ✓	No product	No product
Cs	MeOH/ DMF x	No product	No product	MeOH ✓	No product	No product
Ca	MeOH/ DMF ✓	MeOH/ DMF x	MeOH x	MeOH/ DMF ✓	MeOH/ DMF x	MeOH/ DMF ✓
Sr	MeOH/ DMF ✓✓✓	MeOH/ DMF x	MeOH x	MeOH/ DMF ✓	MeOH/ DMF ✓✓	MeOH/ DMF ✓✓

	MeOH/	MeOH/	MeOH	MeOH/	MeOH/	MeOH/
Ba	DMF	DMF		DMF	DMF	DMF
	✖	✖	✖	✓	✖	✓

MeOH/DMF = successful synthesis route; ✓, ✓✓, ✓✓✓ = outcome of crystal structure determination indicating the number of structures obtained; ✖ = product created, but not isolated or single crystal structure obtained.

3. Group 1 MOF Results

3.1 Single-crystal X-ray diffraction analyses

Single-crystal X-ray diffraction data for **K4_2**, **Rb4_2**, and **Cs4_2** were collected at 293K on a Rigaku AFC12 goniometer equipped with an enhanced sensitivity (HG) Saturn 724+ detector mounted at the window of an FR-E+ Superbright Mo K α rotating anode generator with optics VHF Varimax 70 μ m focus and equipped with an Oxford CryosystemsCobra¹⁹ cooling device. Cell determination, data collection, data reduction, cell refinement and absorption corrections were carried out using CrystalClear-SM Expert 3.1 b27 software²⁰. All structures were solved using Superflip²¹. All structures were refined using full-matrix least-squares refinements in the SHELX2013 software²². All non-hydrogen atoms were refined with anisotropic displacement parameters. All hydrogen atoms were added at calculated positions and refined using a riding model with isotropic displacement parameters based on the equivalent isotropic displacement parameter (Ueq) of the parent atom.

Identification code	K4_2	Rb4_2	Cs4_2
Empirical formula	C ₈ F ₄ K ₂ O ₄	C ₈ F ₄ O ₄ Rb	C ₈ CsF ₄ O ₄
Formula weight	314.28	321.55	368.99
Temperature (K)	293(2)	293(2)	293(2)
Wavelength (Å)	0.71075	0.71075	0.71075
Crystal system	Monoclinic	Monoclinic	Monoclinic
Space group	<i>I</i> 2/m	<i>I</i> 2/a	<i>I</i> 2/a
<i>Unit cell dimensions</i>			
a (Å)	4.03902(2)	9.2821(7)	9.3605(7)
b (Å)	19.9427(18)	9.7189(7)	9.6918(7)
c (Å)	6.0405(4)	10.9837(8)	11.0752(7)
α (°)	90	90	90
β (°)	91.319(8)	110.340(5)	108.566(5)
γ (°)	90	90	90
Volume/Å³	485.45(6)	929.08(12)	952.45(12)
Z	2	4	4
ρcalc (mg/mm³)	2.150	2.299	2.573
Absorption coefficient (mm⁻¹)	1.042	5.394	3.951
F(000)	308	612	684
Crystal	Needle; Colourless	Block; Colourless	Block; Colourless
Crystal size (mm³)	0.120 x 0.010 x 0.010	0.100 x 0.050 x 0.040	0.150 x 0.100 x 0.050
θ range for data collection (°)	3.525 – 27.486	3.142 - 27.313	2.860 - 27.540
Reflections collected	3275	5406	5821
Independent reflections	578 [0.0373]	1045 [0.0665]	1103 [0.0310]
Completeness to θ max	99.6 %	99.8 %	99.9 %
Max and min transmission	1.000 and 0.657	1.000 and 0.661	1.000 and 0.819
Data/restraints/parameters	578 / 0 / 43	1045 / 0 / 78	1103 / 0 / 78
Goodness-of-fit on F2	1.083	1.098	1.097
Final R indexes [$I \geq 2\sigma(I)$]	R1 = 0.0257, wR2 = 0.0724	R1 = 0.0802, wR2 = 0.1850	R1 = 0.0214, wR2 = 0.0559
Final R indexes [all data]	R1 = 0.0298, wR2 = 0.0744	R1 = 0.0837, wR2 = 0.1900	R1 = 0.0214, wR2 = 0.0559
Largest diff. peak/hole (e Å⁻³)	0.267/-0.243	3.634/-0.627	0.687/-0.762
CCDC deposition number/reference code	CCDC-959837/PIPDOJ	1046530	1046529

Table S1 - Group 1 (1,4-fBDC) Products SXRD Data

3.2 Structure Discussion

K4_2

Complex **K4_2**, previously reported by Werker et al., crystallises in the monoclinic $I2/m$ space group as a 3D non-porous metal-organic framework.^[3] The asymmetric unit is made up of one K(I) ion and roughly one quarter fBDC ligand. The K(I) ion is coordinated to six O atoms from five different carboxylate groups (one bidentate ($K1-O1 = 2.862(2)\text{\AA}$) and four monodentate ($K1-O1 = 2.716(2)\text{\AA}$ x2, and $K1-O1 = 2.856(2)\text{\AA}$ x2) associated with the fBDC ligands to form a distorted trigonal prism which is completed by two $K\cdots F$ contacts [$2.840(2)\text{\AA}$] to two of the five coordinating ligands. These distances are in reasonable agreement with the K–O distances found in ionic K₂O ($K-O = 2.787\text{\AA}$) and somewhat longer than the K–F distances found in ionic KF ($K-F = 2.672\text{\AA}$). $K(\text{COO})_5$ link together to create 2D sheets which are cross-linked through the fBDC linkers along the crystallographic b axis creating a 3D structure. This 3D MOF has been determined by PLATON to have no solvent accessible voids.^[4]

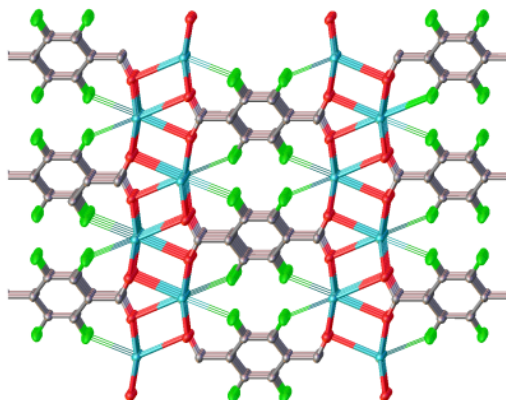


Figure S1 - K4_2 SXRD

Rb4_2/Cs4_2

Both complexes, Rb4_2 and Cs4_2, crystallise in the monoclinic $I2/a$ space group as a 3D non-porous MOF. The asymmetric unit is made up of one Rb/Cs ion, and one quarter fBDC ligand. The Rb(I) ion is coordinated to six O atoms associated with six different carboxylates (all bound in a monodentate fashion ($Rb1-O1 = 3.049(3)\text{\AA}$, x2, $Rb1-O2 = 3.061(5)\text{\AA}$, x2, $Rb1-O2 = 3.070(4)\text{\AA}$, x2) associated with six fBDC ligands forming a distorted trigonal prism which is completed by two $Rb\cdots F$ contacts [$3.179(3)\text{\AA}$] to two of the six coordinating ligands. $Rb(\text{COO})_6$ link together to create 2D sheets which are cross-linked by the fBDC linkers along the crystallographic c axis creating a 3D structure.

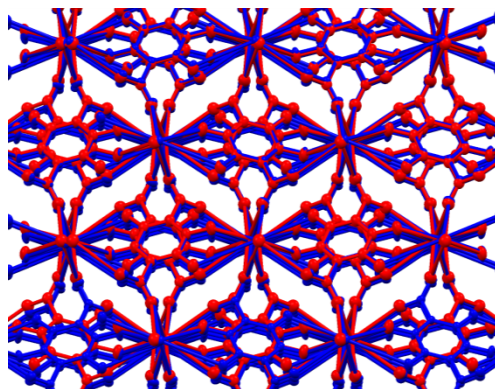


Figure S2 - Rb4_2/Cs4_2 SXRD

3.3 Powder X-ray diffraction analyses

The Bruker D2 Phaser benchtop powder XRD system (which uses a (30kv, 10mA) Cu ($K\alpha_1/K\alpha_2$) radiation source and a Ni $K\beta$ filter (detector side), additional beam optics and settings: primary and secondary axial Soller slits (2.5°), fixed 0.6mm divergence slit, 1mm anti-scatter-screen, detector: 1D LYNXEYE with a 5° window) was used to analyse each MOF product. The samples were collected using a Si low background sample holder (20mmx0.5mm sample cavity) to minimise background noise. The scans were collected over a 2theta range of $5-60^\circ$ at 1 sec/step with 1097 steps in total. Each scan taking 20 mins using DIFFRAC.SUITE COMMANDER software.

K4_2 observed vs. calc.

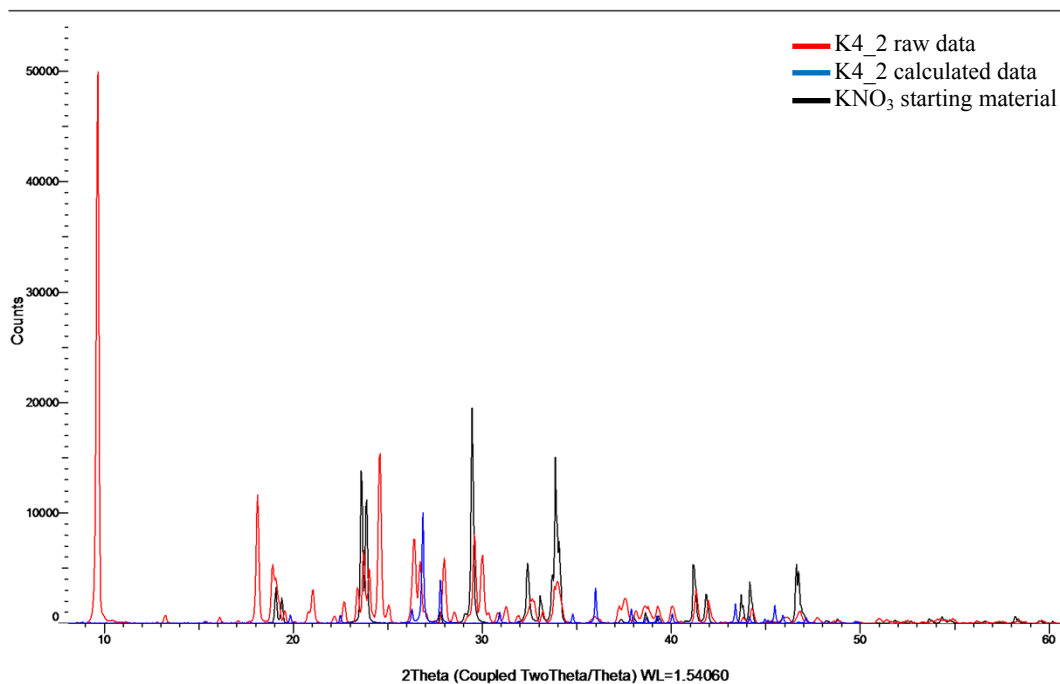


Figure S3 - K4_2 PXRD observed vs calculated (with Potassium nitrate overlaid)

Within K4_2 there is an additional unidentified component present within the bulk sample.

Rb4_2 observed vs. calc.

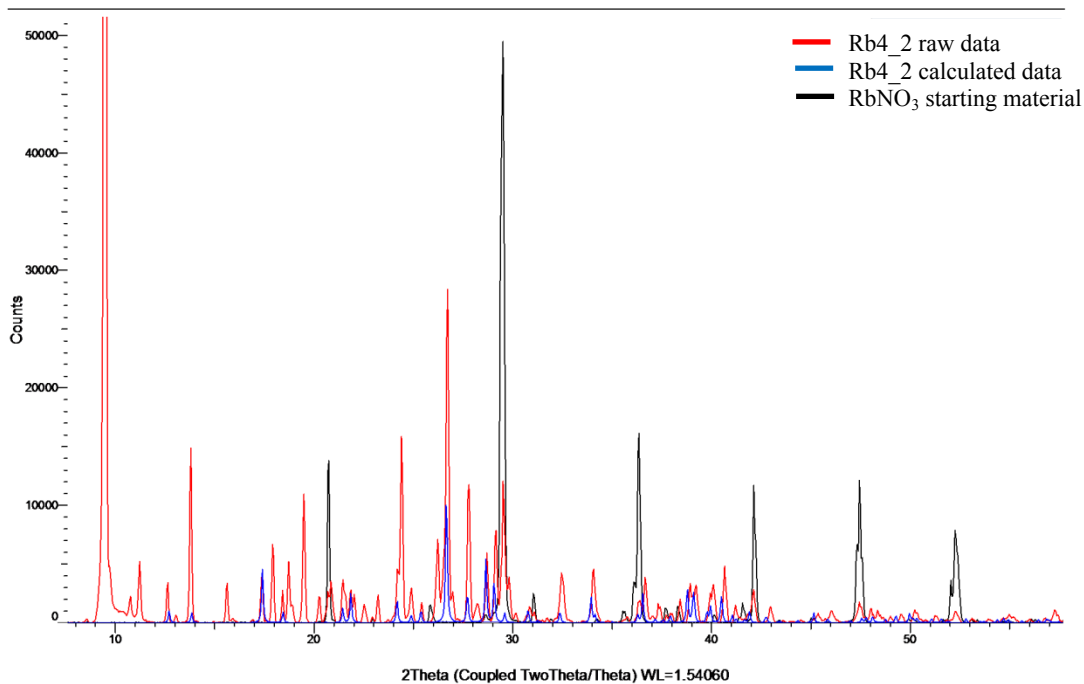


Figure S4 - Rb4_2 PXRD observed vs calculated (with Rubidium nitrate overlaid)

Cs4_2 observed vs. calc.

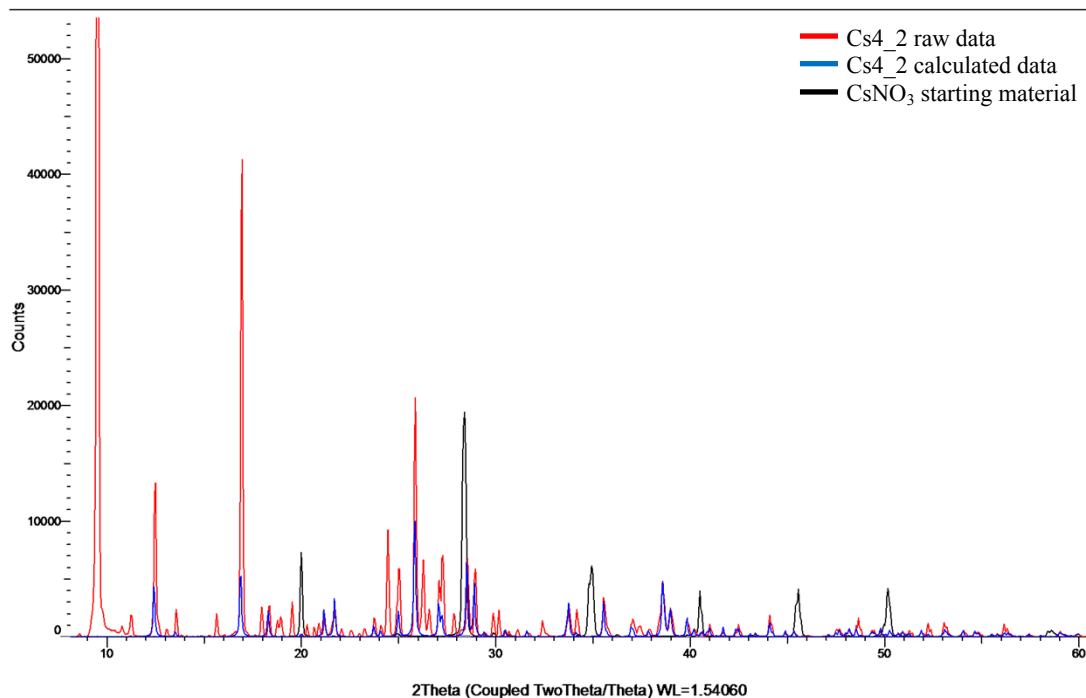


Figure S5 - Cs4_2 PXRD observed vs calculated (with Cesium nitrate overlaid)

Rubidium nitrate and cesium nitrate products PXRD patterns were overlaid to further emphasise the observations made from overlaying the structures in Mercury where these structures were seen to be isostructural. This is clearly evident from the PXRD patterns (Figure S5 and S6). There is an additional isostructural component present seen in the observed patterns for both Rb_fBDC and Cs_fBDC as can be seen in Figure S5 where there are peaks appearing before a 2Theta value of 10°.

Rb fBDC overlaid with Cs fBDC

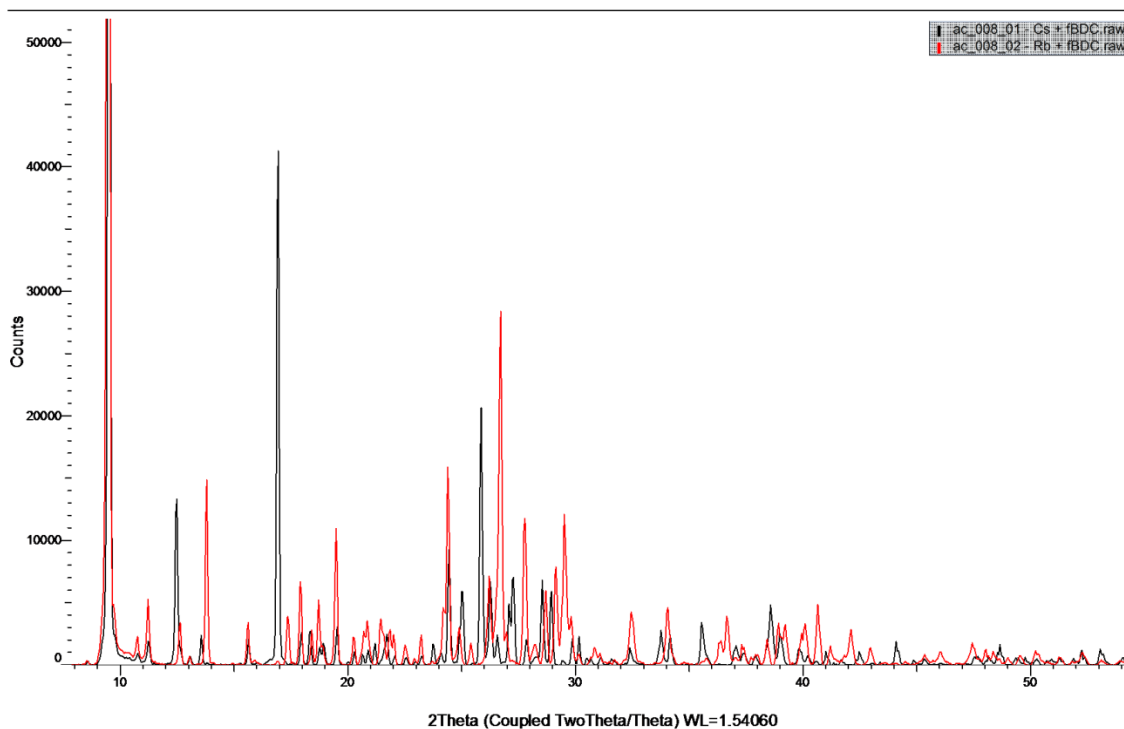


Figure S6 - Rb4_2 vs Cs4_2 observed

Rb4_2 vs. Cs4_2 calculated data comparison

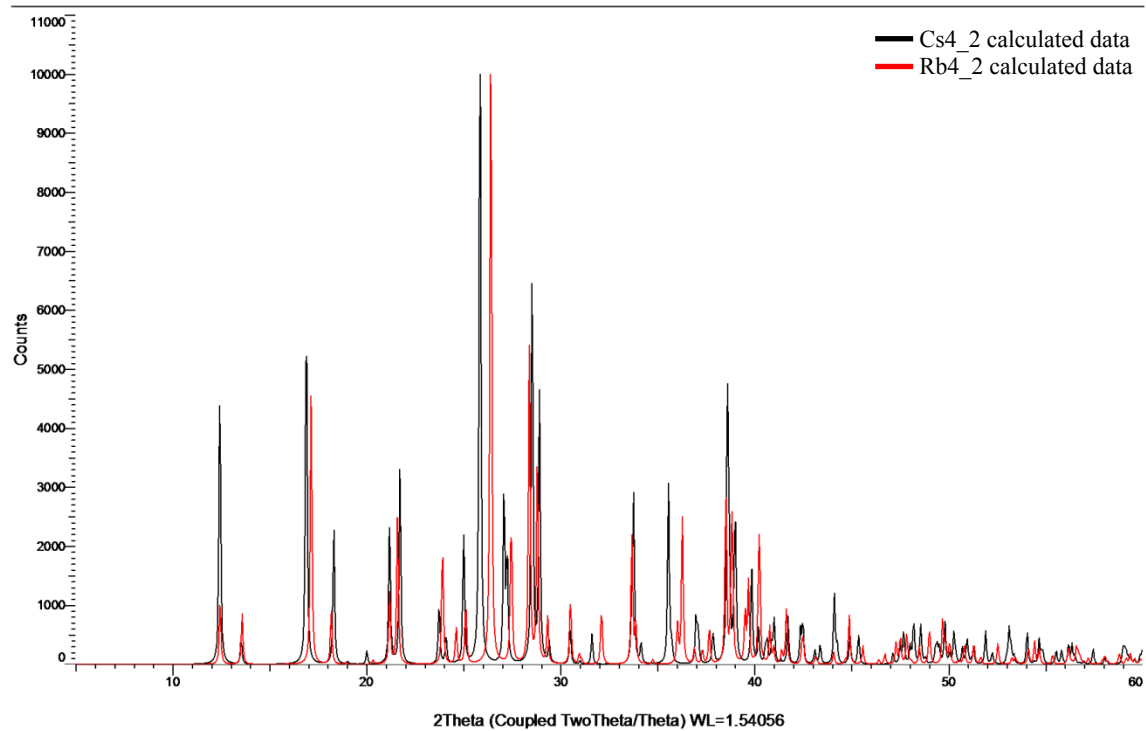


Figure S7 - Rb4 2 vs Cs4 2 calculated

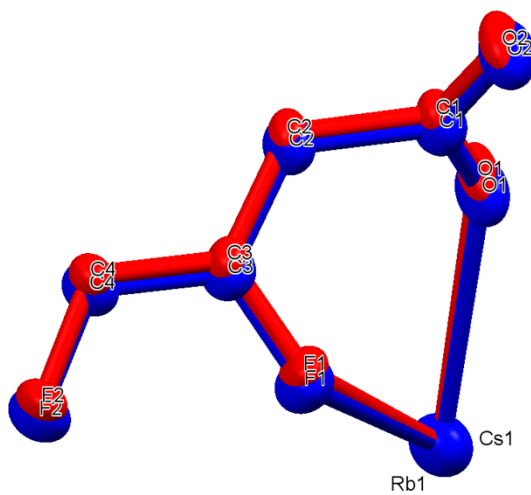


Figure S8 - Structure overlay of Rb4 2 and Cs4 2 in Mercury (Rb = red, Cs = Blue)

3.4 DSC Traces (under nitrogen)

The thermal analysis of each Group 1 product coupled with 1,4-fBDC was carried out using a Mettler-Toledo differential scanning calorimeter instrument, model DSC821e, equipped with a liquid nitrogen low temperature attachment and a TSO801RO Universal sample robot (heating rate: $10^{\circ}\text{Cmin}^{-1}$; the flow rate of nitrogen gas: 40ml/min; the sample size: 4 – 10mg in 40 μl aluminium dishes).

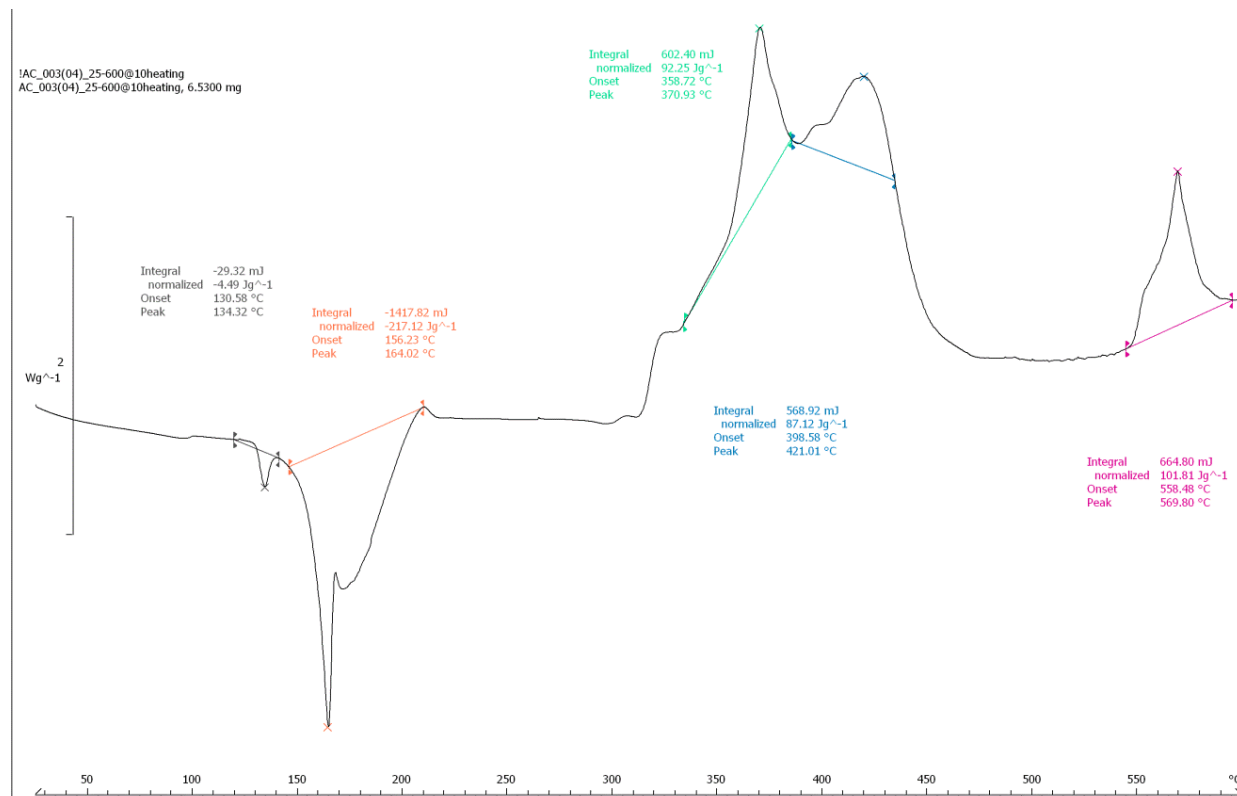


Figure S9 – K4_2_DSC trace

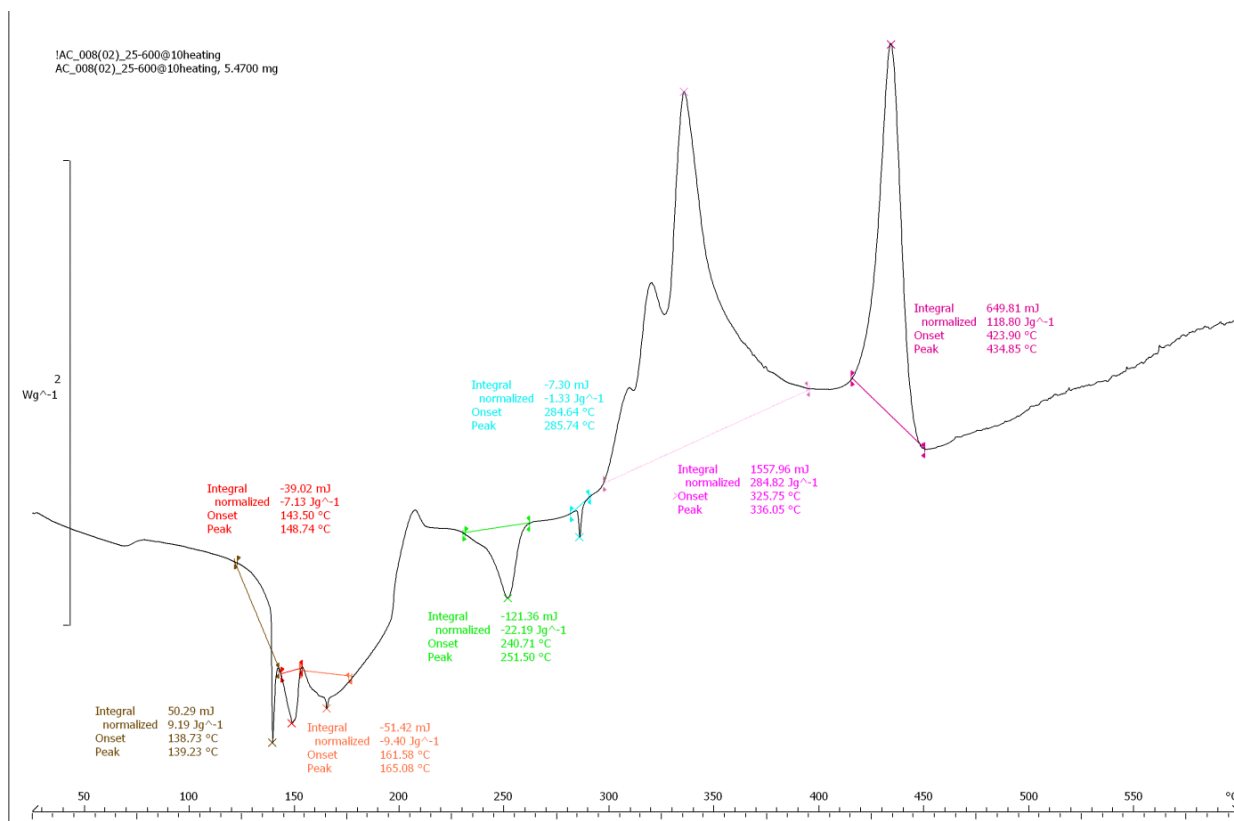


Figure S10 – Rb4_2 DSC trace

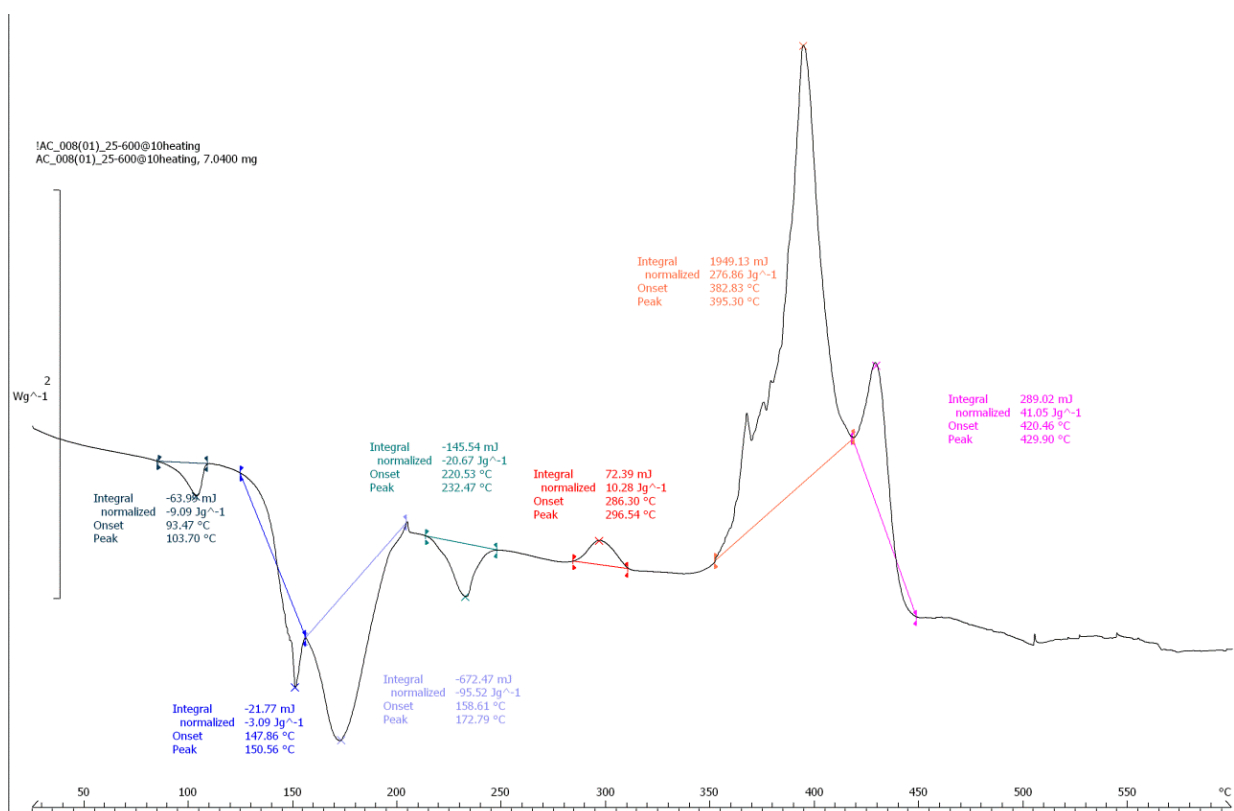


Figure S11 – Cs4_2 DSC trace

3.5 Burn Tests

The alkaline earth metal MOFs were burn tested within a fume hood on top of a heat proof mat which had a small enclosure mounted on top of it to minimise the effects of the airflow on the burn test. Approximately 15mg of sample was placed onto a heat proof tile and ignited using a blow torch. Photographs were taken by Sharif Ahmed using a Canon EOS 7D camera (exposure 1/100 sec).



Figure S12 - Burn Test of K4_2



Figure S13 - Burn Test of Rb4_2



Figure S14 - Burn Test of Cs4_2

4. Group 2 MOF Results

4.1 Single-crystal X-ray diffraction analyses

Single-crystal X-ray diffraction data for **Ba4_1/2**, **Ca4_2**, **Sr4_2**, **Sr5_1**, **Sr5_2**, **Ca6_2**, **Sr6_1**, **Sr6_2**, and **Ba6_2** were collected at 100K on a Rigaku AFC12 goniometer equipped with an enhanced sensitivity (HG) Saturn 724+ detector mounted at the window of an FR-E+ Superbright Mo K α rotating anode generator with optics VHF Varimax 70 μ m focus and equipped with an Oxford CryosystemsCobra¹⁹ cooling device. Cell determination, data collection, data reduction, cell refinement and absorption corrections were carried out using CrystalClear-SM Expert 3.1 b27 software.²⁰ Both **Ca6_2** and **Sr6_2** were processed using CrysAlis Pro (Agilent Technologies V1.171.37.35).^[5] All structures were solved using Superflip²¹. All structures were refined using full-matrix least-squares refinements in the SHELX2013 software²². All non-hydrogen atoms were refined with anisotropic displacement parameters. All hydrogen atoms were added at calculated positions and refined using a riding model with isotropic displacement parameters based on the equivalent isotropic displacement parameter (Ueq) of the parent atom.

Identification code	Ba4_1/2	Ca4_2	Sr4_2
Empirical formula	C ₁₆ H ₂ Ba ₂ F ₈ O ₉	C ₁₃ H ₈ CaF ₄ N ₂ O ₈	C ₁₃ H ₈ SrF ₄ N ₂ O ₈
Formula weight	764.86	436.29	483.83
Temperature (K)	100(2)	100(2)	100(2)
Wavelength (Å)	0.71075	0.71075	0.71075
Crystal system	Monoclinic	Orthorhombic	Orthorhombic
Space group	C2/c	Pna21	Pna21
<i>Unit cell dimensions</i>			
a (Å)	12.5647(9)	14.2384(10)	14.2686(10)
b (Å)	7.1406(5)	16.3862(11)	16.7326(11)
c (Å)	19.8230(14)	6.8450(5)	7.0181(5)
α (°)	90	90	90
β (°)	101.663(2)	90	90
γ (°)	90	90	90
Volume/Å³	1741.8(2)	1597.03(19)	1675.6(2)
Z	4	4	4
ρ_{calc} (mg/mm³)	2.917	1.815	1.918
Absorption coefficient (mm⁻¹)	4.637	0.488	3.309
F(000)	1416	880	952
Crystal	Plate; Colourless	Block; Colourless	Plate; Colourless
Crystal size (mm³)	0.040 x 0.030 x 0.010	0.070 x 0.060 x 0.040	0.110 x 0.040 x 0.030
θ range for data collection (°)	3.299 – 27.483	2.861 – 27.487	2.822 – 27.529
Reflections collected	10971	19489	17674
Independent reflections	2001 [0.0504]	3646 [0.0518]	3743 [0.0589]
Completeness to θ max	99.9 %	99.7 %	98.3 %
Max and min transmission	1.000 and 0.737	1.000 and 0.779	1.000 and 0.794
Data/restraints/parameters	2001 / 0 / 159	3646 / 1 / 258	3743 / 1 / 257
Goodness-of-fit on F2	1.043	1.042	1.030
Final R indexes [$I \geq 2\sigma(I)$]	R1 = 0.0222, wR2 = 0.0536	R1 = 0.0354, wR2 = 0.0913	R1 = 0.0372, wR2 = 0.1031
Final R indexes [all data]	R1 = 0.0259, wR2 = 0.0554	R1 = 0.0366, wR2 = 0.0923	R1 = 0.0377, wR2 = 0.1038
Largest diff. peak/hole (e Å⁻³)	0.897/-0.687	0.458/-0.213	0.659/-0.489
CCDC deposition number/reference code	1046526	1046528	1046533

Identification code	Sr5_1	Sr5_2	Ca6_2
Empirical formula	C ₁₁ H ₁₅ F ₄ NO ₉ Sr	C ₁₃ H ₈ F ₄ N ₂ O ₈ Sr	C ₁₃ H ₆ CaF ₄ N ₂ O ₇
Formula weight	468.86	483.83	418.28
Temperature (K)	100(2)	100(2)	100(2)
Wavelength (Å)	0.71075	0.71075	0.71075
Crystal system	Triclinic	Triclinic	Monoclinic
Space group	<i>P</i> −1	<i>P</i> −1	<i>P</i> 2 ₁ / <i>n</i>
<i>Unit cell dimensions</i>			
a (Å)	8.8263(7)	7.3008(5)	4.4398(3)
b (Å)	8.9293(7)	9.1264(5)	23.0380(18)
c (Å)	10.8630(9)	13.1904(9)	14.3878(9)
α (°)	92.612(16)	101.118(6)	90
β (°)	93.939(17)	93.830(5)	96.661(6)
γ (°)	100.991(18)	110.526(6)	90
Volume/Å³	836.95(13)	798.95(9)	1461.69(17)
Z	2	2	4
ρ_{calc} (mg/mm³)	1.860	2.011	1.901
Absorption coefficient (mm^{−1})	3.311	3.469	0.524
F(000)	468	476	840
Crystal	Plate; Colourless	Block; Colourless	Needle; Colourless
Crystal size (mm³)	0.060 × 0.040 × 0.010	0.140 × 0.040 × 0.020	0.130 × 0.010 × 0.010
θ range for data collection (°)	2.899 – 27.554	3.012 – 27.488	1.677 – 27.483
Reflections collected	11298	10036	18914
Independent reflections	3861 [0.1280]	3656 [0.0868]	3350 [0.1066]
Completeness to θ max	99.8 %	99.7 %	100.0 %
Max and min transmission	1.000 and 0.289	1.000 and 0.253	1.000 and 0.221
Data/restraints/parameters	3861 / 0 / 243	3656 / 0 / 254	3350 / 0 / 248
Goodness-of-fit on F²	1.009	1.036	1.095
Final R indexes [I>=2σ (I)]	R1 = 0.0858, wR2 = 0.2044	R1 = 0.0574, wR2 = 0.1482	R1 = 0.0594, wR2 = 0.1281
Final R indexes [all data]	R1 = 0.1114, wR2 = 0.2221	R1 = 0.0605, wR2 = 0.1525	R1 = 0.1085, wR2 = 0.1623
Largest diff. peak/hole (e Å^{−3})	2.981/−1.807	1.667/−2.458	0.550/−0.636
CCDC deposition number/reference code	1046534	1046535	1046527

Identification code	Sr6_1	Sr6_2	Ba6_2*
Empirical formula	C ₁₁ H ₁₀ F ₄ NO ₆ Sr	C ₄₂ H ₂₀ F ₁₆ N ₂ O ₂₀ Sr ₃	C ₂₆ H ₁₈ Ba ₂ F ₈ N ₂ O ₁₁
Formula weight	415.82	1439.46	961.10
Temperature (K)	100(2)	100(2)	100(2)
Wavelength (Å)	0.71075	0.71075	0.71075
Crystal system	Triclinic	Monoclinic	Monoclinic
Space group	<i>P</i> -1	<i>C</i> 2	<i>P</i> 2 ₁ / <i>n</i>
<i>Unit cell dimensions</i>			
a (Å)	6.1469(4)	32.076(3)	7.0904(5)
b (Å)	7.0452(5)	6.1638(3)	32.270(2)
c (Å)	16.1438(11)	11.5618(7)	7.2698(5)
α (°)	94.495(16)	90	90
β (°)	96.741(16)	97.569(7)	117.997(2)
γ (°)	101.639(17)	90	90
Volume/Å³	676.26(9)	2266.0(3)	1468.72(17)
Z	2	2	2
ρ_{calc} (mg/mm³)	2.042	2.110	2.173
Absorption coefficient (mm⁻¹)	4.067	3.672	2.781
F(000)	410	1408	920
Crystal	Needle; Colourless	Plate; Colourless	Prism; Colourless
Crystal size (mm³)	0.040 × 0.020 × 0.010	0.160 × 0.030 × 0.010	0.040 × 0.020 × 0.010
θ range for data collection (°)	3.106 – 27.473	1.777 – 27.545	2.525 – 27.483
Reflections collected	7817	14120	17867
Independent reflections	3016 [0.1512]	5028 [0.0584]	3366 [0.0663]
Completeness to θ max	99.1 %	99.9 %	99.9 %
Max and min transmission	1.000 and 0.468	1.000 and 0.423	1.000 and 0.769
Data/restraints/parameters	3016 / 0 / 211	5028 / 328 / 376	3366 / 0 / 239
Goodness-of-fit on F²	0.989	1.160	1.037
Final R indexes [I>=2σ (I)]	R1 = 0.1003, wR2 = 0.1915	R1 = 0.0838, wR2 = 0.2130	R1 = 0.0360, wR2 = 0.0814
Final R indexes [all data]	R1 = 0.1912, wR2 = 0.2308	R1 = 0.0906, wR2 = 0.2190	R1 = 0.0477, wR2 = 0.0867
Largest diff. peak/hole (e Å⁻³)	1.294/−0.754	1.908/−2.311	0.732/−1.031
CCDC deposition number/reference code	1046531	1046532	1046525

Table S2 - Group 2 Fluorinated Products SXRD Data

*Ba6_2 - Ba atoms are disordered over two positions. Due to this it is impossible to model the exact positions of the lighter atoms resulting in some close contacts that can safely be ignored.

4.2 Structure Discussion

Ba4_1/2

Complex Ba4_1/2 crystallises in the monoclinic C2/c space group as a 3D non-porous metal-organic framework. The asymmetric unit is made up of one Ba(II) atom, two half 1,4-fBDC ligands and one coordinated water. The Ba ion is coordinated to seven O ions from six carboxylate groups (one bidentate and five monodentate) associated with the fBDC ligands and one water O ion. One carboxylate (O1—C1—O2) is bidentate to one barium and monodentate to two others. The other carboxylate (O11—C11—O12) is monodentate to three bariums. One of the oxygens, O12, is monodentate to one barium ion whilst the other, O11, is monodentate to two. The Ba coordination geometry is that of a distorted dodecahedron, a common structure for eight-coordinate metal ions. Ba-O bond distances range from 2.686(2) – 2.957(2) Å. These values are comparable to those listed for Ba-O (carboxylate) and Ba-O (aqua) bonds in other eight coordinate barium coordination polymers.^[6] Ba(OH₂)(COO)₆ link together to create 2D sheets which are cross-linked through the 1,4-fBDC linkers along the crystallographic c axis. The 1,4-fBDC linkers lie roughly parallel to one another between each sheet but on moving from one sheet to the next they rotate by 73°. Each Ba(II) acts as a node joining four COO groups. One carboxylate bridges two adjacent Ba(II) ions whilst the other bridges three. This 3D MOF has been determined by PLATON to have no solvent accessible voids.^[4] This structure was particularly interesting as the same product resulted irrespective of the synthesis method chosen.

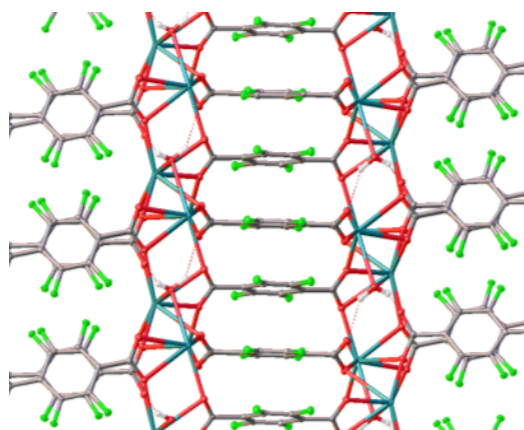


Figure S15 - Ba4_2 SXR

Ca4_2/Sr4_2

Complexes Ca4_2 and Sr4_2 crystallise in the orthorhombic Pna2₁ space group as 3D porous metal-organic frameworks. The asymmetric unit is made up of a Ca/Sr(II) atom, one 1,4-fBDC ligand, a nitrate anion, a coordinated water molecule and pyridine solvent. The Ca/Sr(II) atom is coordinated to six O atoms from four carboxylate groups (two bidentate (O1, O2, O3, O4) and two monodentate (O1, O2) associated with the 1,4-fBDC ligands, one O from a nitrate anion (O13), and one O from a coordinated water (O1W). The Ca(II) coordination geometry is that of a biaugmented triangular prism. Ca-O bond distances range from 2.395(2) – 2.618(2) Å (Sr = 2.488(4) – 2.726(3) Å). These values are comparable to those listed for Ca-O/Sr-O (carboxylate) and Ca-O/Sr-O (aqua) bonds in other eight coordinate calcium/strontium coordination polymers.^[7] Ca/Sr(OH₂)(COO)₄ link together to create 1D chains which are cross-linked through 1,4-fBDC linkers in two directions to create a 3D MOF. Pyridine resides in the pores of this structure.

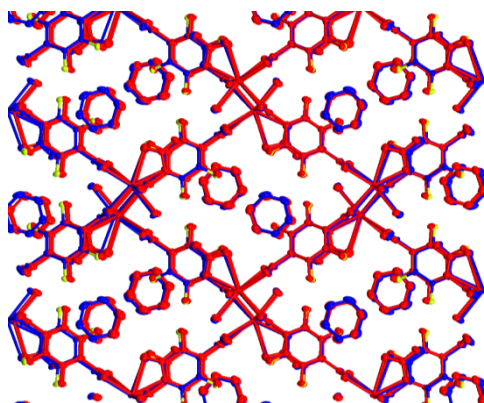


Figure S16 - Ca4_2/Sr4_2 SXR

Sr5_1

Sr5_1 crystallises in the triclinic P-1 space group. It is composed of 1D chains constructed from Sr ions linked by 1,3-fBDC ligands. The asymmetric unit consists of one Sr ion, one 1,3-fBDC ligand, one coordinated DMF molecule, three coordinated water molecules and one solvent water molecule. Sr is in an eight coordinate system with biaugmented triangular prism geometry. Sr is bonded in a bidentate fashion to one iso fBDC ligand (O1, O2) and monodentate to two other 1,3-fBDC ligands (O1, O3), three coordinated water molecules (O1W, O2W, O3W), and one coordinated DMF molecule (O1S). Sr-O bond distances range from 2.499(5) – 2.750(5) Å. These values are comparable to those listed for Sr-O (carboxylate) and Sr-O (aqua) bonds in other eight coordinate strontium coordination polymers.^[7d] Sr(OH₂)₃(DMF)(COO)₃ chains which form along crystallographic *a* axis are extended into a 2D supramolecular network by means of hydrogen bonding which takes place between coordinated water molecules.

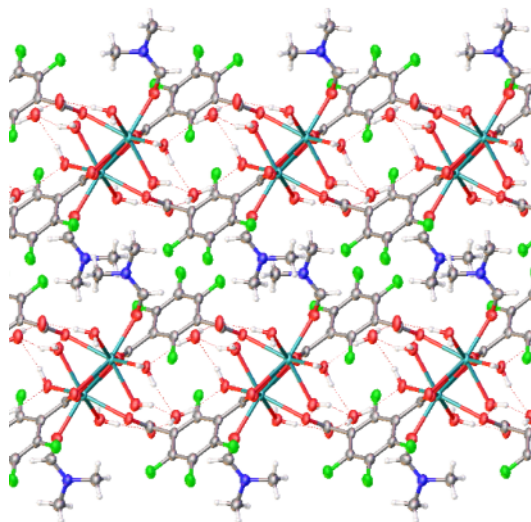


Figure S17 - Sr5_1 SXRD

Sr5_2

Sr5_2 crystallises in the orthorhombic Pna21 space group consisting of 2D sheets constructed from Sr ions linked by 1,3-fBDC ligands. The asymmetric unit consists of one Sr ion, one 1,3-fBDC ligand, one nitrate anion, and one coordinated water molecule. Sr is in a nine coordinate system with pentagonal bipyrid geometry. One carboxylate from the 1,3-fBDC ligands is μ -bridged to two different Sr ions whilst the other carboxylate is bidentate to another Sr ion and monodentate to two others. Sr is bonded in a bidentate fashion to one 1,3-fBDC ligand (O1, O2), and one nitrate anion (O11, O12), and is monodentate to four 1,3-fBDC ligands (O1, O2, O3, O4) and one coordinated water molecule (O1W). Sr-O bond distances range from 2.572(3) – 2.780(3) Å. These values are comparable to those listed for Sr-O (carboxylate) and Sr-O (aqua) bonds in other nine coordinate strontium coordination polymers.^[7d] Sr(OH₂)(COO)₅(NO₃) chains link together to create 2D sheets by the cross-linking of the isofBDC linkers along the crystallographic *a* axis. Between the 2D sheets lie pyridine molecules which are stabilised by hydrogen bonding to coordinated water molecules (O1W-H1Wa..N1S).

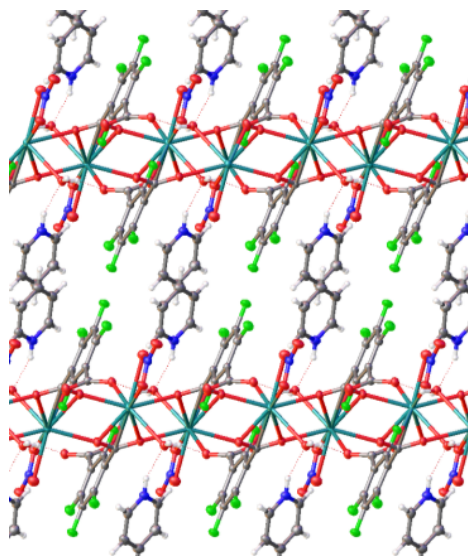


Figure S18 - Sr5_2 SXR

Ca6_2

Ca6_2 crystallised in the monoclinic P21/n space group. The asymmetric unit consists of a Ca ion, one 1,2-fBDC ligand, one nitrate anion, and one pyridine solvent molecule. Ca is bonded in a bidentate fashion to one 1,2-fBDC ligand (O3, O4) and a nitrate anion (O11, O12), and monodentate bound to four 1,2-fBDC ligands (O1, O2, O2, O4). Ca is in an eight coordinate system with biaugmented triangular prism geometry. Ca-O bond distances range from 2.373(3) – 2.509(3)Å. These values are comparable to those listed for Ca-O(carboxylate) bonds in other eight coordinate calcium coordination polymers.^[7]Ca(COO)₅(NO₃) units link together to form 1D chains along the crystallographic *a* axis. The protonated pyridine molecules hydrogen bond to one of the oxygen atoms from the nitrate anions, O12.

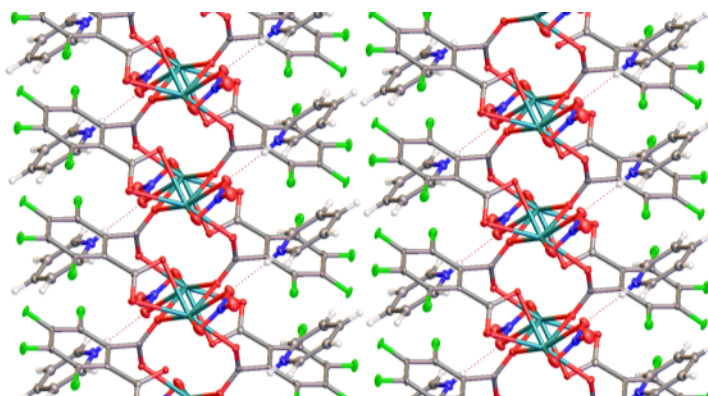


Figure S19 - Ca6_2 SXR

Sr6_1

Sr6_1 crystallises in the triclinic P-1 space group. The asymmetric unit consists of one Sr ion, one 1,2-fBDC ligand, one coordinated water molecule, and one coordinated DMF molecule. One carboxylate from the 1,2-fBDC ligands is μ -bridged to two different Sr ions whilst the other carboxylate is bidentate to another Sr ion and monodentate to two others. Sr is in an eight coordinate system with biaugmented triangular prism geometry. Sr is bonded in a bidentate fashion to one 1,2-fBDC ligand (O1, O2), and is monodentate to four 1,2-fBDC ligands (O1, O2, O3, O4), one coordinated water molecule (O1W) and one DMF molecule (O1S). Sr-O bond distances range from 2.481(7) – 2.777(8)Å. These values are comparable to those listed for Sr-O (carboxylate) and Sr-O (aqua) bonds in other eight coordinate strontium coordination polymers.^[7d] Sr(OH₂)(COO)₅(NO₃) chains link together to create 2D sheets by cross-linking 1,2-fBDC linkers along the crystallographic *b* axis. The coordinated water provides additional support to one of the oxygens from the μ -bridging carboxylate (O1W-H1Wa...O3).

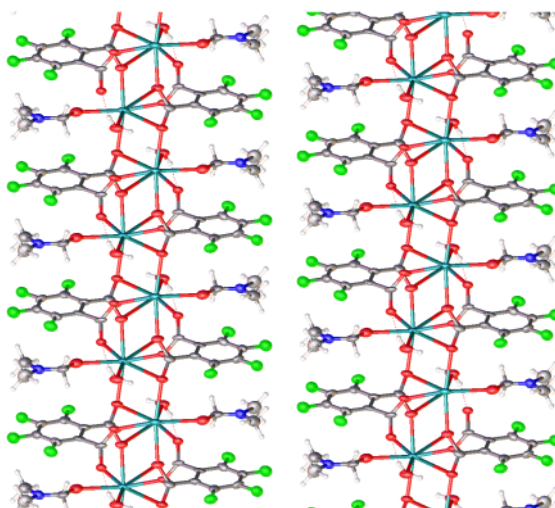


Figure S20 - Sr6_1 SXR

Sr6_2

Sr6_2 crystallised in the monoclinic space group $C2$. There are two unique Sr environments. The asymmetric unit consists of two Sr ions, two 1,2-fBDC ligand, two coordinated water molecules and one pyridine solvent molecule. Sr1 is chelated to two equivalent 1,2-fBDC ligands (O12 x2, O14x2). It is also monodentate bound to two other 1,2-fBDC ligands (O3x2) and two equivalent coordinated water molecules (O1Wx2). Sr2 is chelated to only one 1,2-fBDC (O2, O4) whilst also binding in a bidentate fashion to another 1,2-fBDC (O13, O14). It is also bound to two other inequivalent 1,2-fBDC ligands (O1, O11) and two coordinated water molecules (O1W, O2W). Both Sr cations are eight coordinate with biaugmented triangular prism geometry. Sr-O bond distances range from 2.520(12) – 2.708(13)Å. $\text{Sr}(\text{OH}_2)_2(\text{COO})_6$ chains link together to create 2D sheets by cross-linking of 1,2-fBDC ligands along the crystallographic c axis.

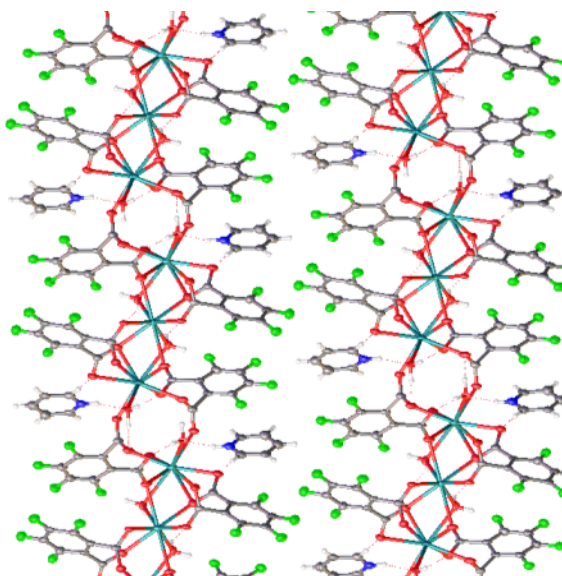


Figure S21 - Sr6_2 SXR

Ba6_2

Ba6_2 crystallises in the monoclinic $P2_1/n$ space group consisting of 2D sheets, composed of Ba ion, 1,2-fBDC ligands and coordinated water molecules. The asymmetric unit consists of one Ba ion which is disordered over two positions, one 1,2-fBDC ligand, coordinated water molecules, and one pyridine molecule which is coordinated in one part of structure but is uncoordinated in the other. Both carboxylates associated with the 1,2-fBDC ligands μ -bridge to two different Ba ions each. One of the carboxylates additionally binds in a bidentate fashion to another Ba. Ba is in a nine coordinate system with triaugmented triangular prism geometry. Ba is bonded in a bidentate fashion to one 1,2-fBDC ligand (O1, O2) and bonded in a monodentate fashion to three others (O1, O2, O3, O4). In one part the Ba ion is coordinated to three water molecules whereas in the other it is coordinated to two water molecules and a pyridine molecule. Ba-O bond distances range from 2.610(2) – 2.997(3) Å. These values are comparable to those listed for Ba-O (carboxylate) and Ba-O(aqua) in other nine coordinate barium coordination polymers.^[8] Ba(OH₂)₃(COO)₅ chains link together to create 2D sheets down crystallographic b axis.

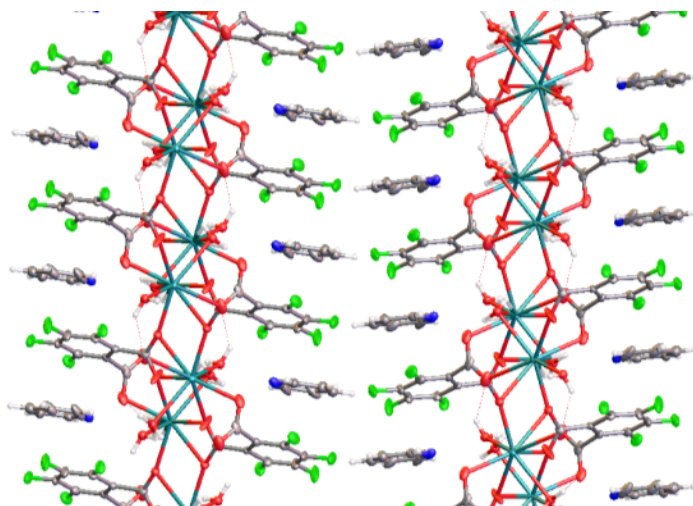


Figure S22 - Ba6_2 SXRD

4.3 Powder X-ray diffraction analyses

The Bruker D2 Phaser benchtop powder XRD system (which uses a (30kv, 10mA) Cu ($K\alpha_1/K\alpha_2$) radiation source and a Ni $K\beta$ filter (detector side), additional beam optics and settings: primary and secondary axial Soller slits (2.5°), fixed 0.6mm divergence slit, 1mm anti-scatter-screen, detector: 1D LYNXEYE with a 5° window) was used to analyse each MOF product. The samples were collected using a Si low background sample holder (20mmx0.5mm sample cavity) to minimise background noise. The scans were collected over a 2theta range of 5 - 60° at 1 sec/step with 1097 steps in total. Each scan taking 20 mins using DIFFRAC.SUITE COMMANDER software.^[9]

Ca1_2 observed vs. calc.

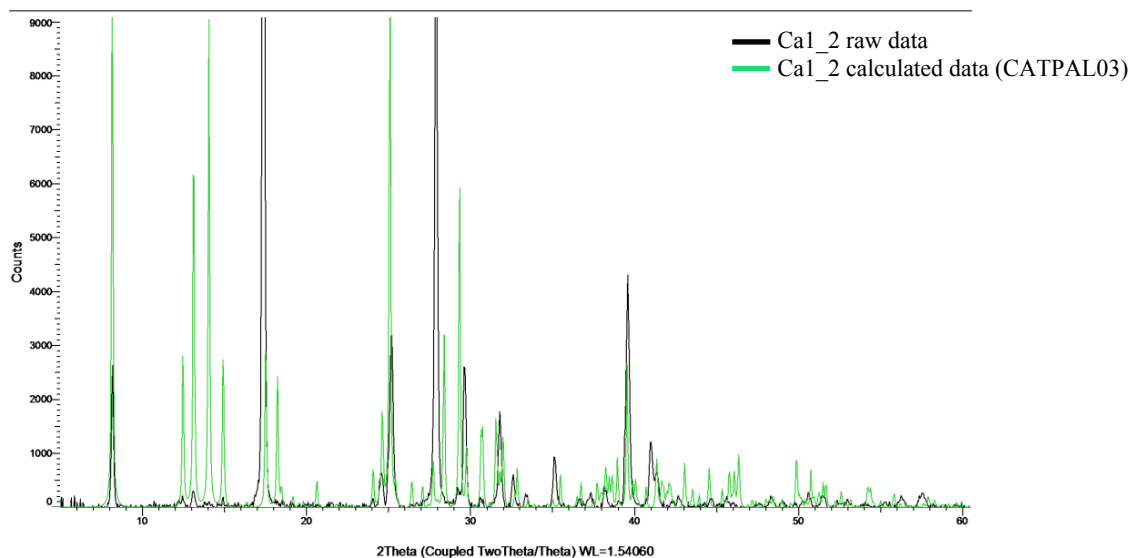


Figure S23 - Ca1_2 (CATPAL03)

Sr1_1 observed vs. calc.

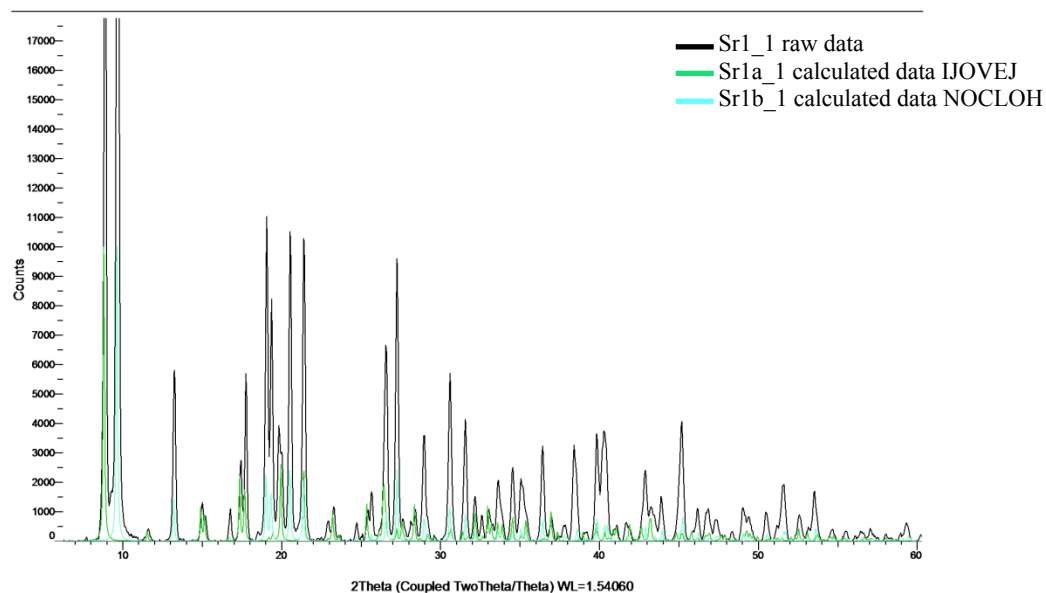


Figure S24 - Sr1_1 (IJOVEJ + NOCLOH)

Sr1_2 observed vs. calc.

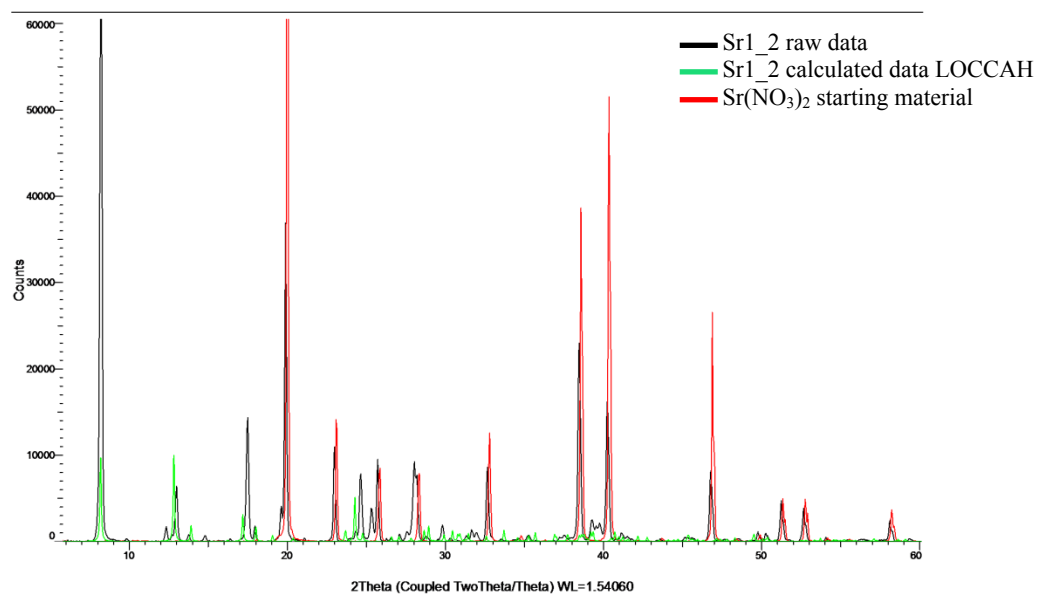


Figure S25 - Sr1_2 (LOCCA and SM overlay)

Ba1_2 product overlay with starting material

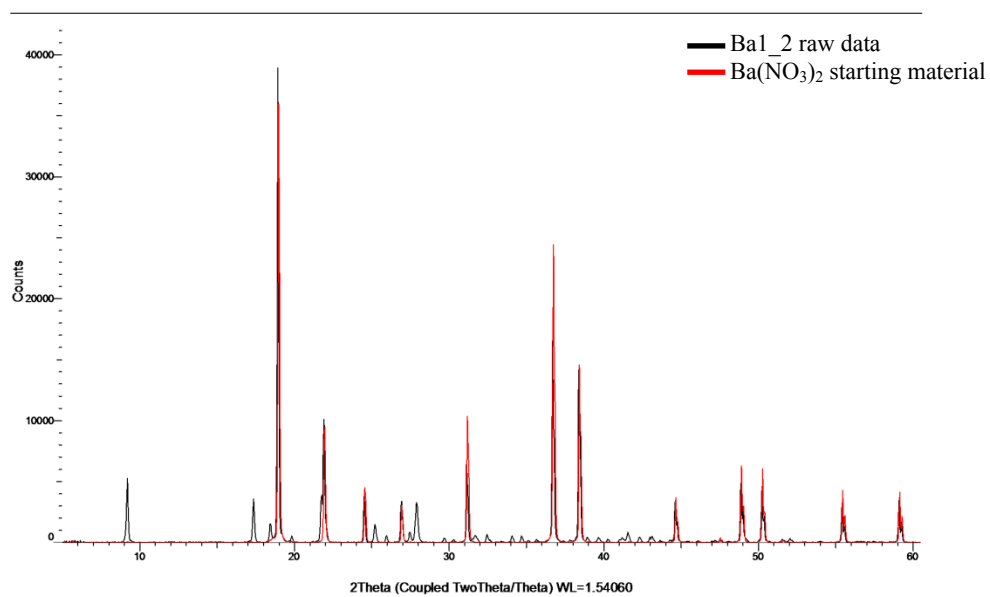


Figure S26 - Ba1_2 Starting Material Overlay

Ba4_1 observed vs. calc.

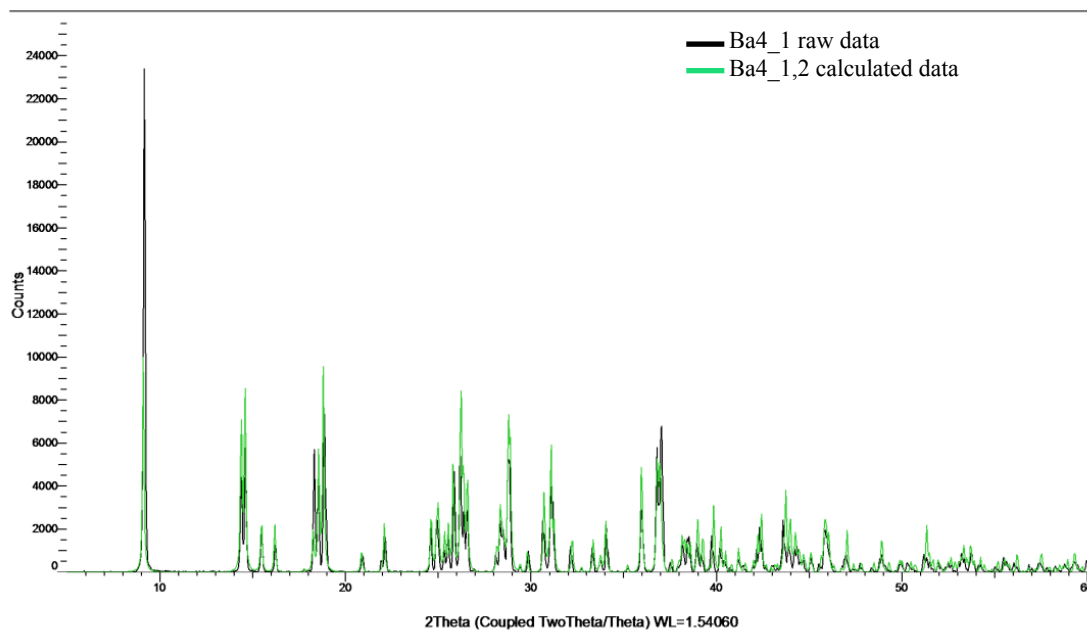


Figure S27- Ba4_1 observed vs calculated

Ba4_2 observed vs. calc.

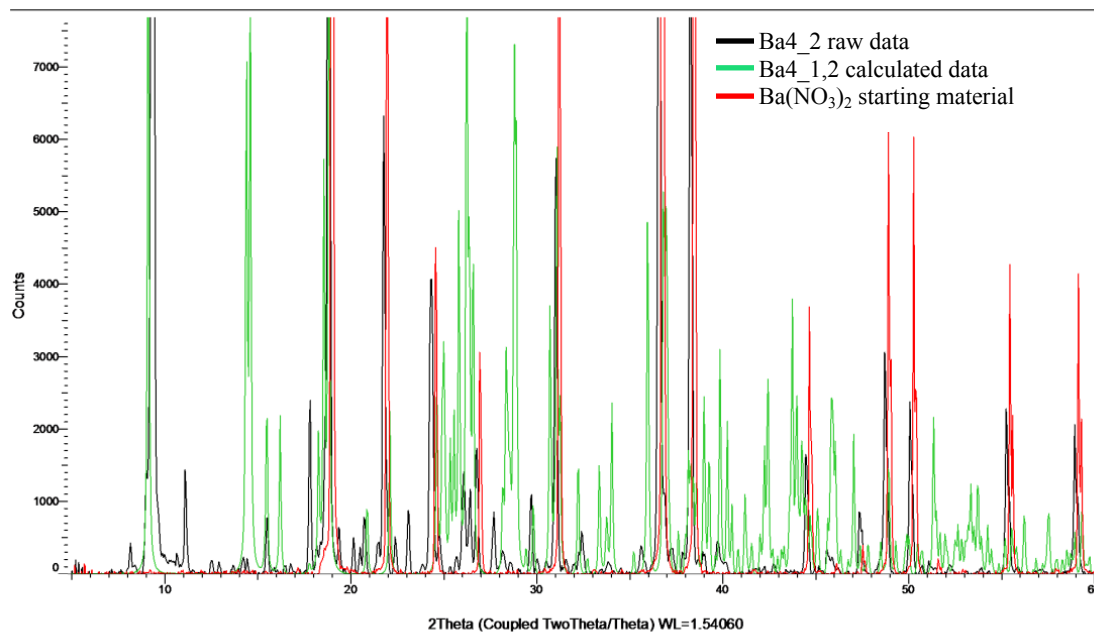


Figure S28 - Ba4_2 observed vs calculated

As can be seen in Figure S27 the calculated pattern and the observed pattern match up perfectly for the Ba fBDC products resulting from the use of the DMF method. It is clear that when using the MeOH approach there is a large amount of unreacted barium nitrate still present. There was no appearance of the oxidisers within the MeOH synthesis for the calcium nitrate and strontium nitrate products. (Figures S29 and S30).

Ca4_2 observed vs. calc.

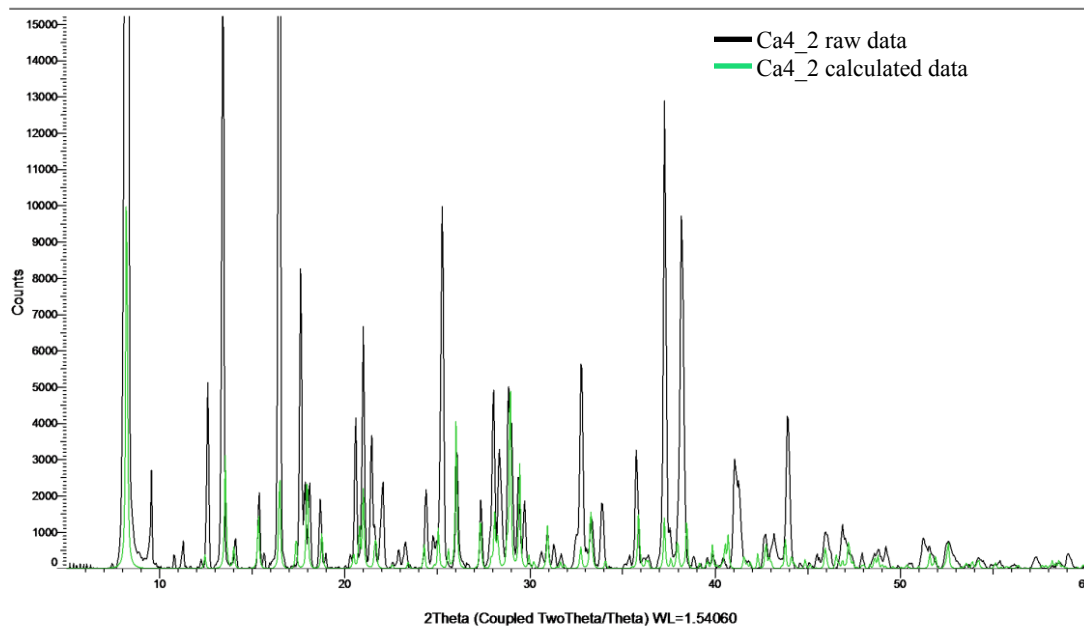


Figure S29 - Ca4_2 observed vs calculated

Sr4_2 observed vs. calc.

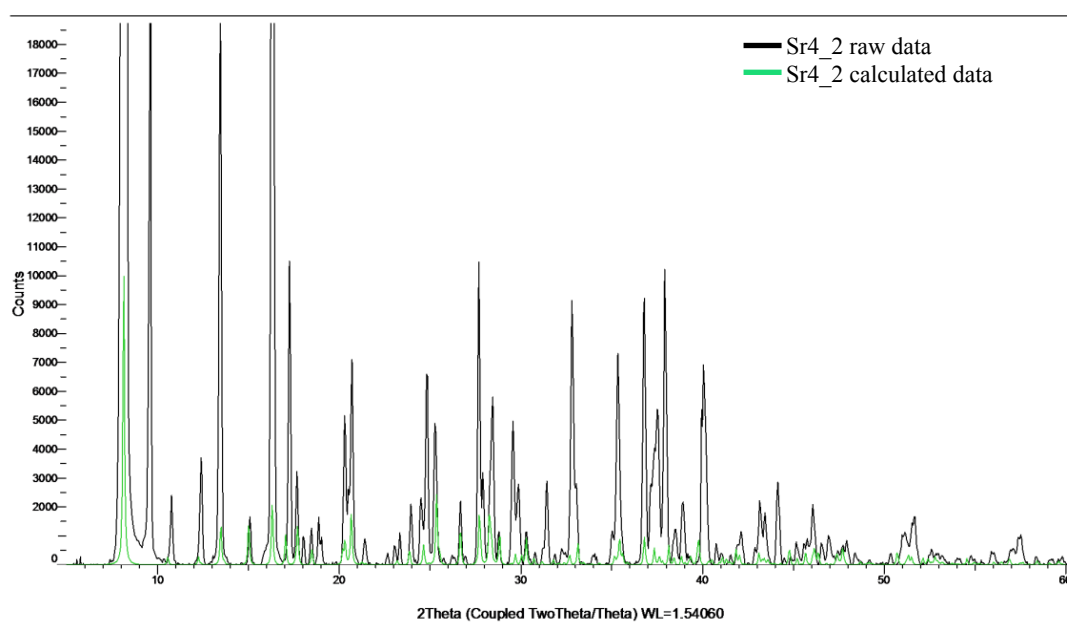


Figure S30 - Sr4_2 observed vs calculated

Calcium nitrate and strontium nitrate products PXRD patterns were overlaid to further emphasise the observations made from overlaying the structures in Mercury (Figure S33) where these structures were seen to be isostructural. This is evident from the PXRD patterns (Figure S31 and S32).

Ca4_2 vs. Sr4_2 raw data comparison

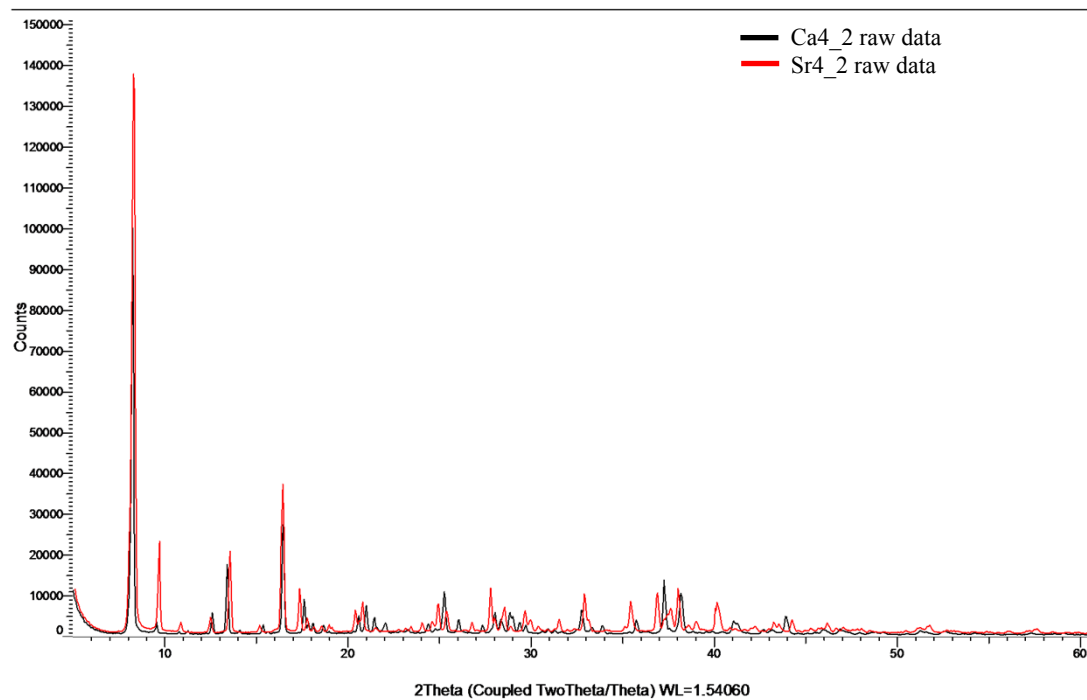


Figure S31 - Ca4_2 vs Sr4_2 observed

Ca4_2 vs. Sr4_2 calculated data comparison

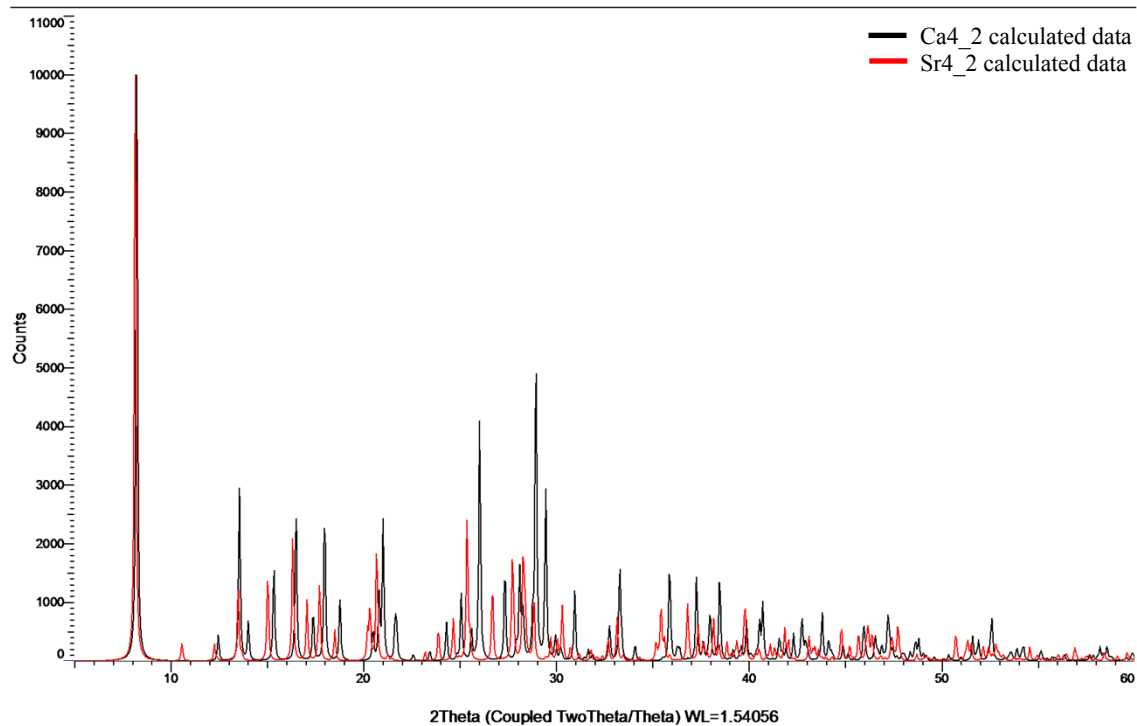


Figure S32 - Ca4_2 vs Sr4_2 calculated

Sr5_2 observed vs. calc.

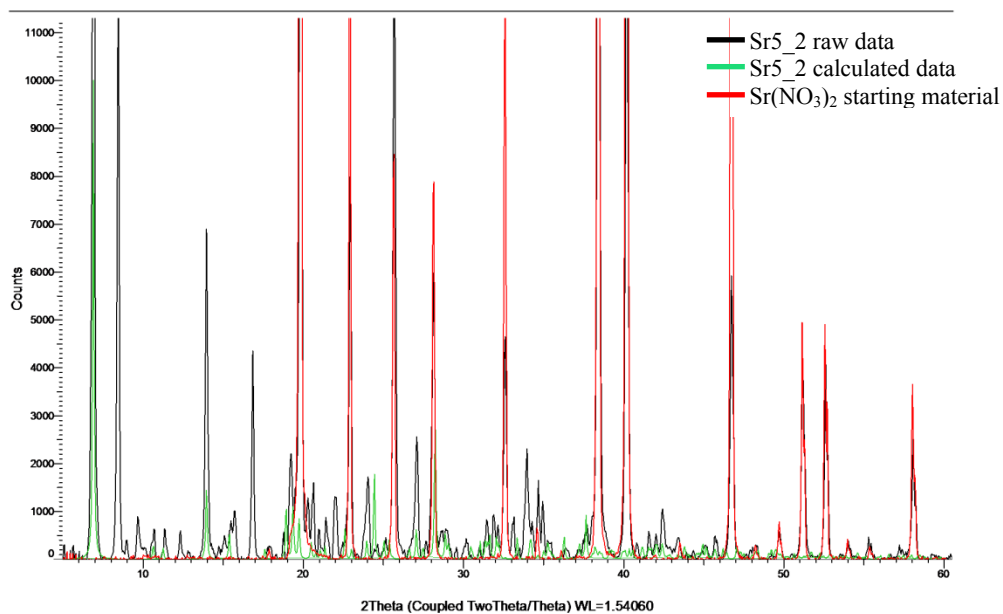


Figure S35- Sr5_2 Product and Starting Material Overlay

The bulk material for Sr5_2 comprises of new product and oxidiser starting material. It additionally contains another unidentified microcrystalline component.

Ca6_2 observed vs. calc.

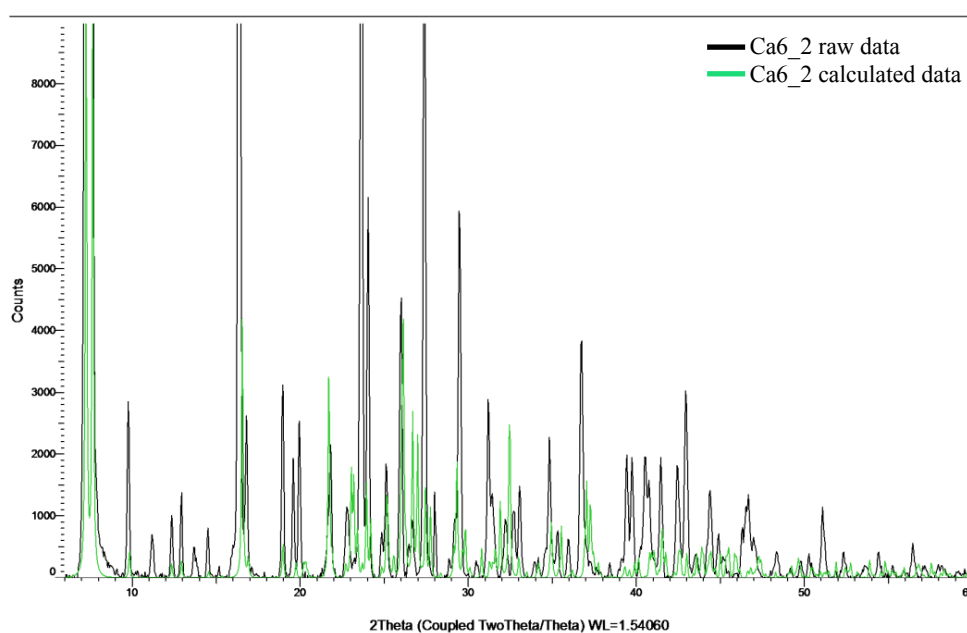


Figure S36 - Ca6_2 Product Overlay

This PXRD pattern suggests that the resultant product is pure.

Sr6_1 observed vs. calc.

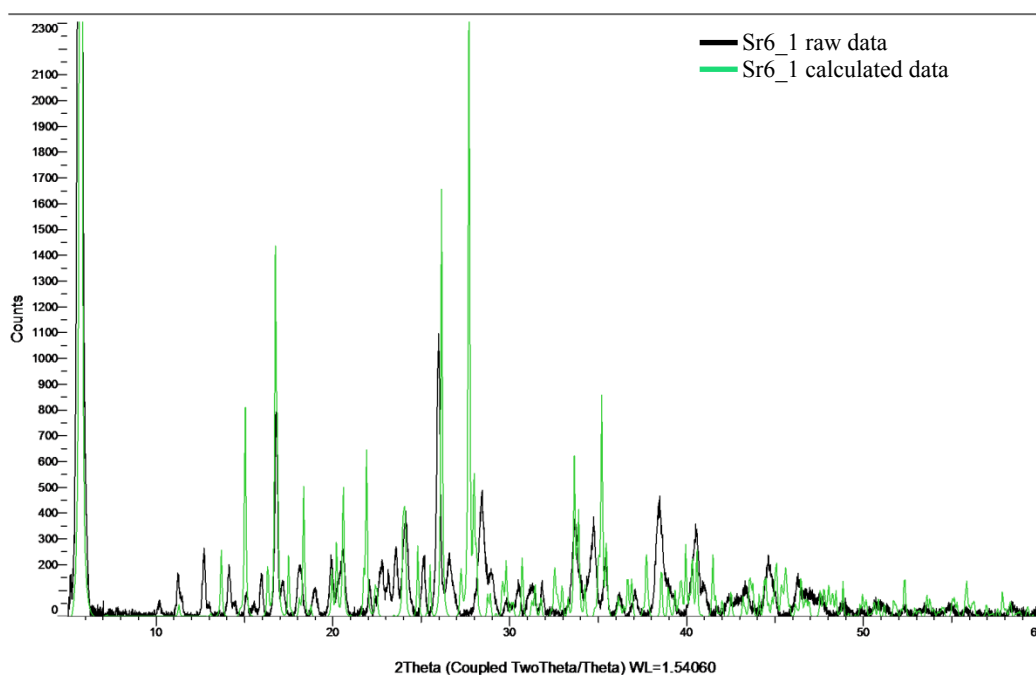


Figure S37 - Sr6_1 Product Overlay

This PXRD pattern also suggests a high level of purity.

Sr6_2 observed vs. calc.

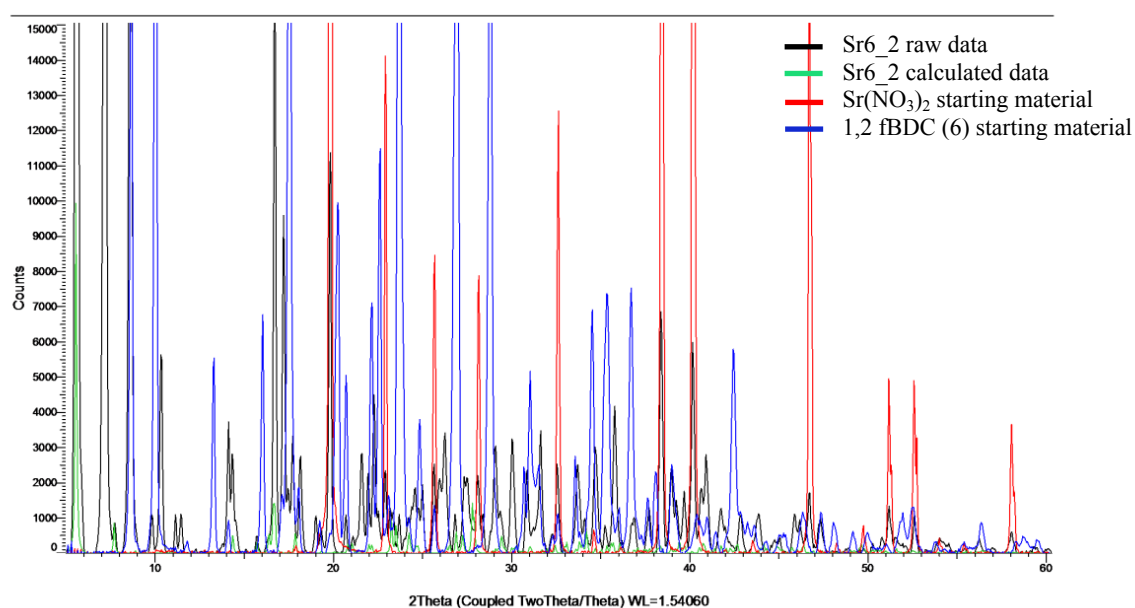


Figure S38 - Sr6_2 Product and Starting Material Overlay

Sr6_2 PXRD pattern is both a mixture of starting materials and new products. Only one of these new products could be identified by SXRD.

Ba6_2 observed vs. calc.

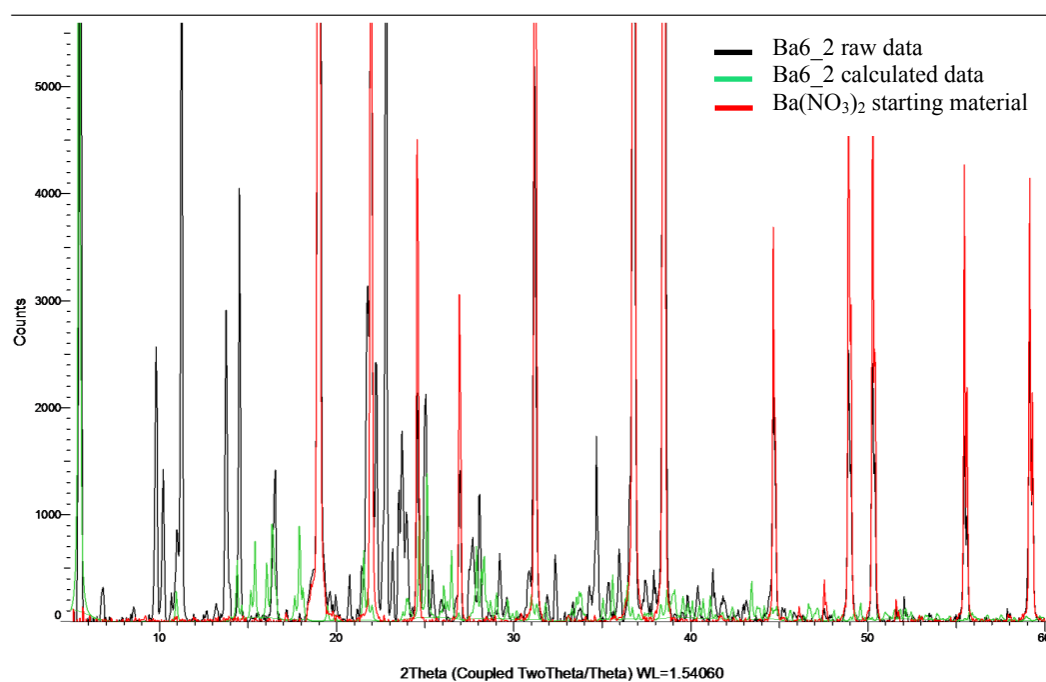


Figure S39 - Ba6_2 Product and Starting Material Overlay

Ba6_2 comprises of new product and oxidiser starting material.

The other crystal structures which formed in combination with the fluorinated linkers could not be characterised by SXRD but their PXRD patterns suggest new products have resulted.

Ca4_1 observed vs. calc.

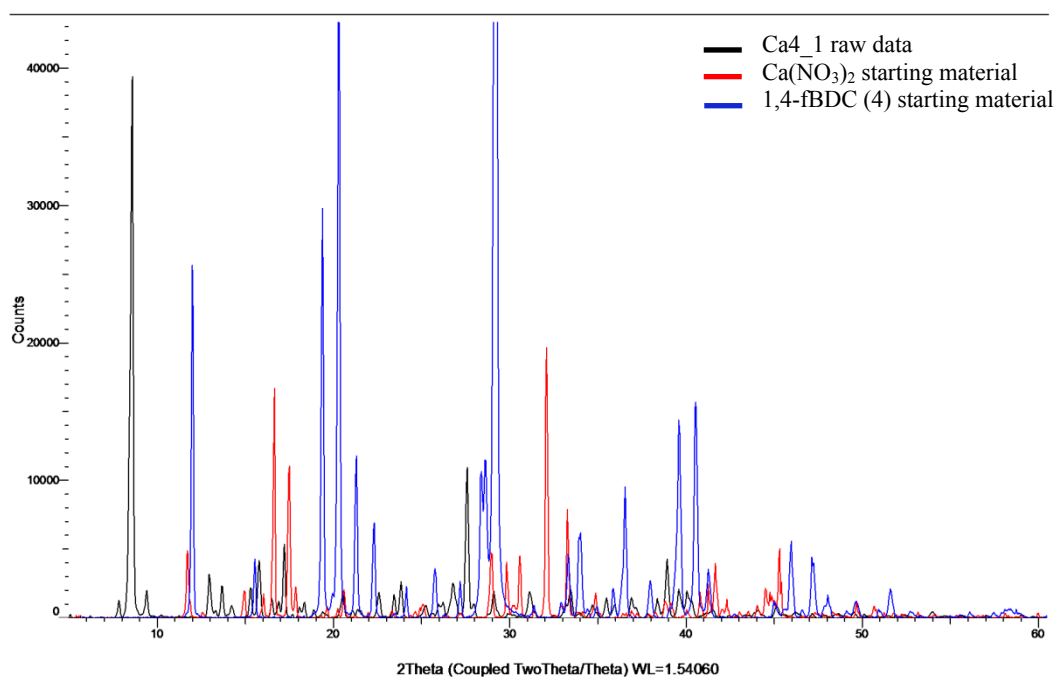


Figure S40 - Ca4_1 Starting Material Overlay

Sr4_1 observed vs. calc.

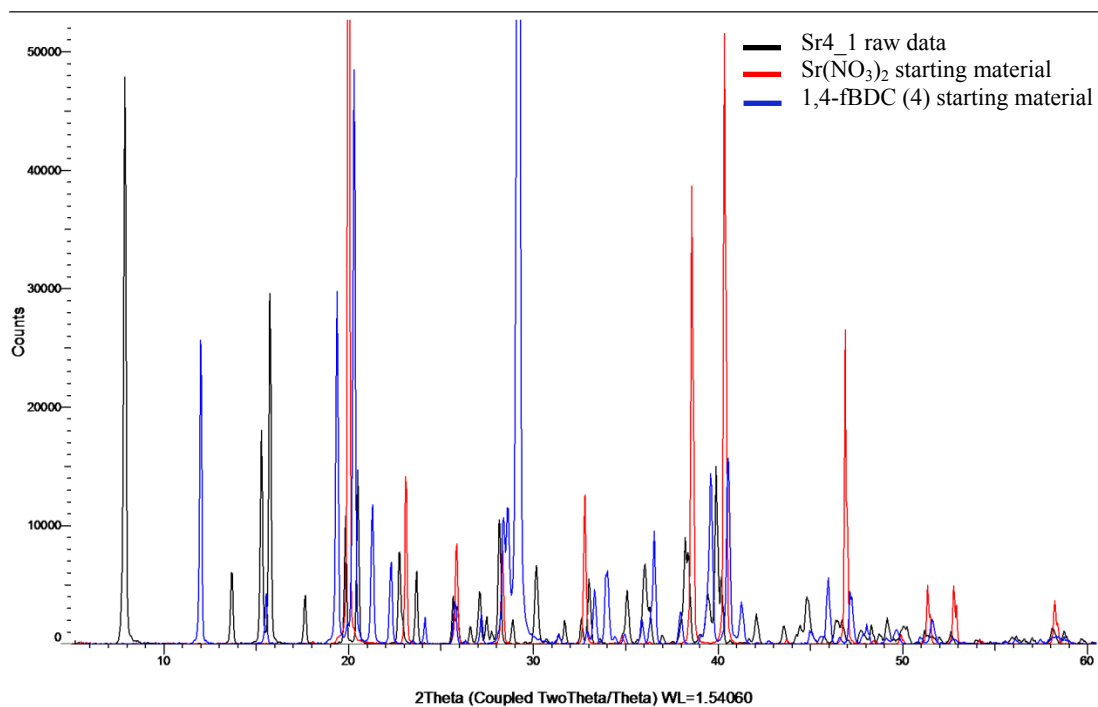


Figure S41 - Sr4_1 Starting Material Overlay

Ca5_1 observed vs. calc.

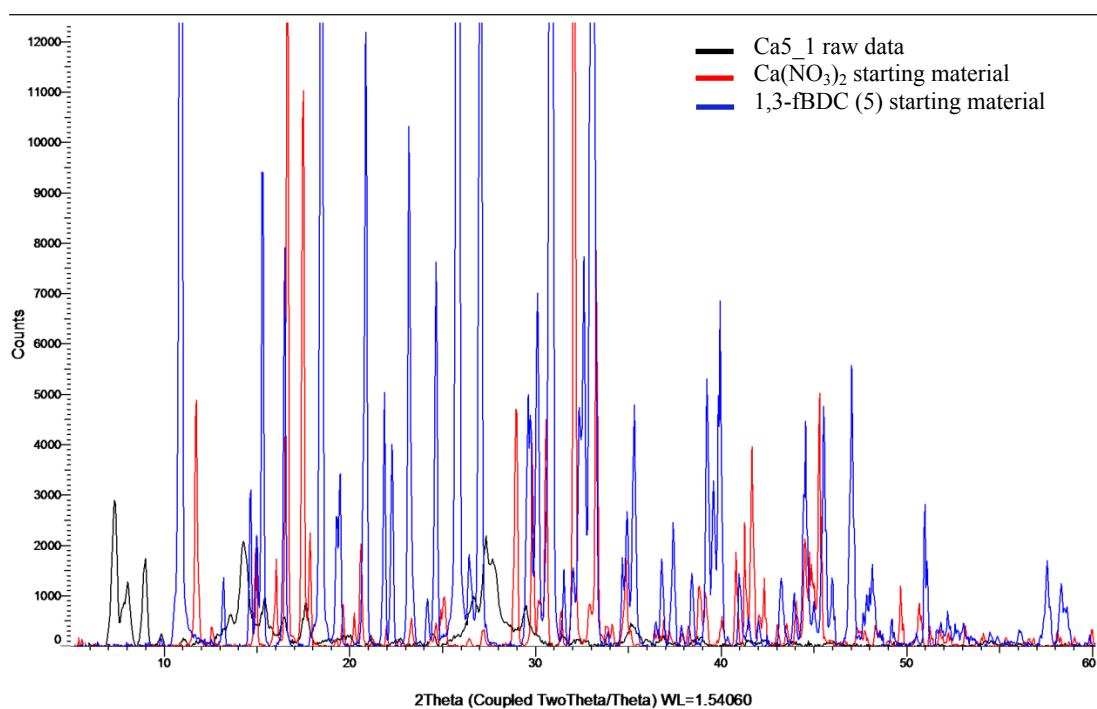


Figure S42 - Ca5_1 Starting Material Overlay

Ca5_2 observed vs. calc.

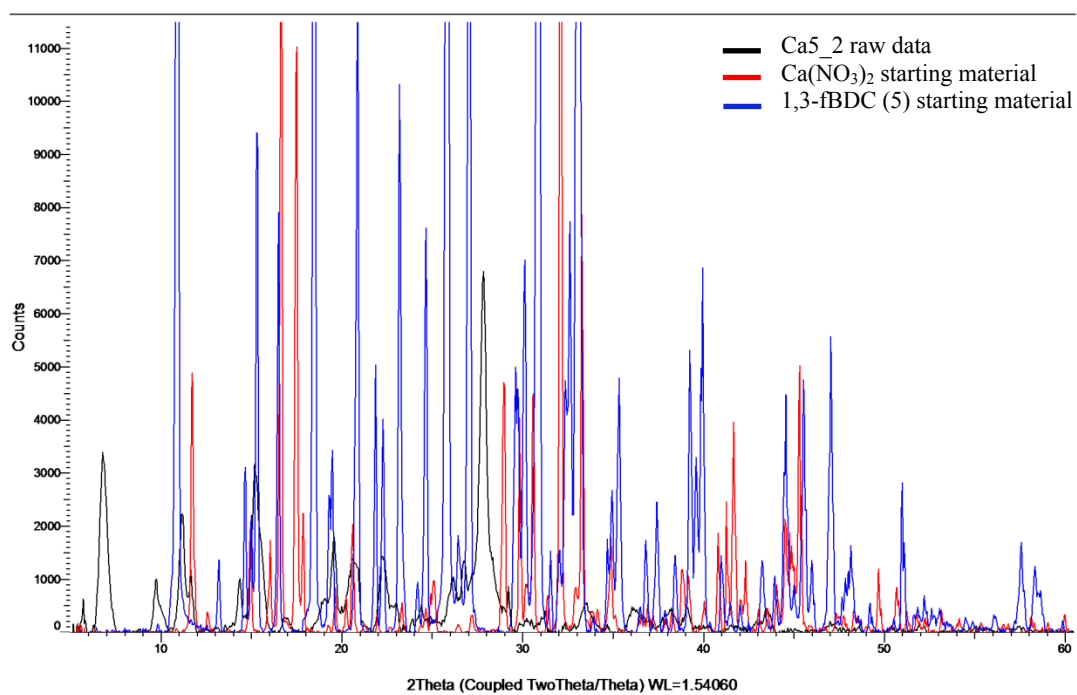


Figure S43 - Ca5_2 Starting Material Overlay

Ba5_1 observed vs. calc.

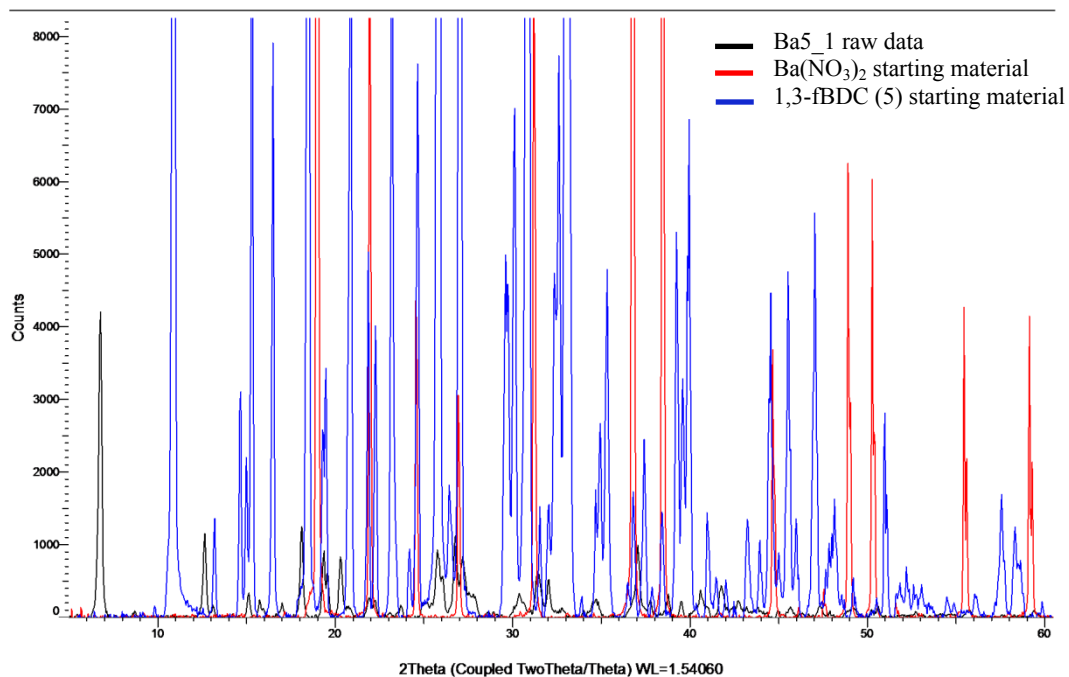


Figure S44 - Ba5_1 Starting Material Overlay

Ba5_2 observed vs. calc.

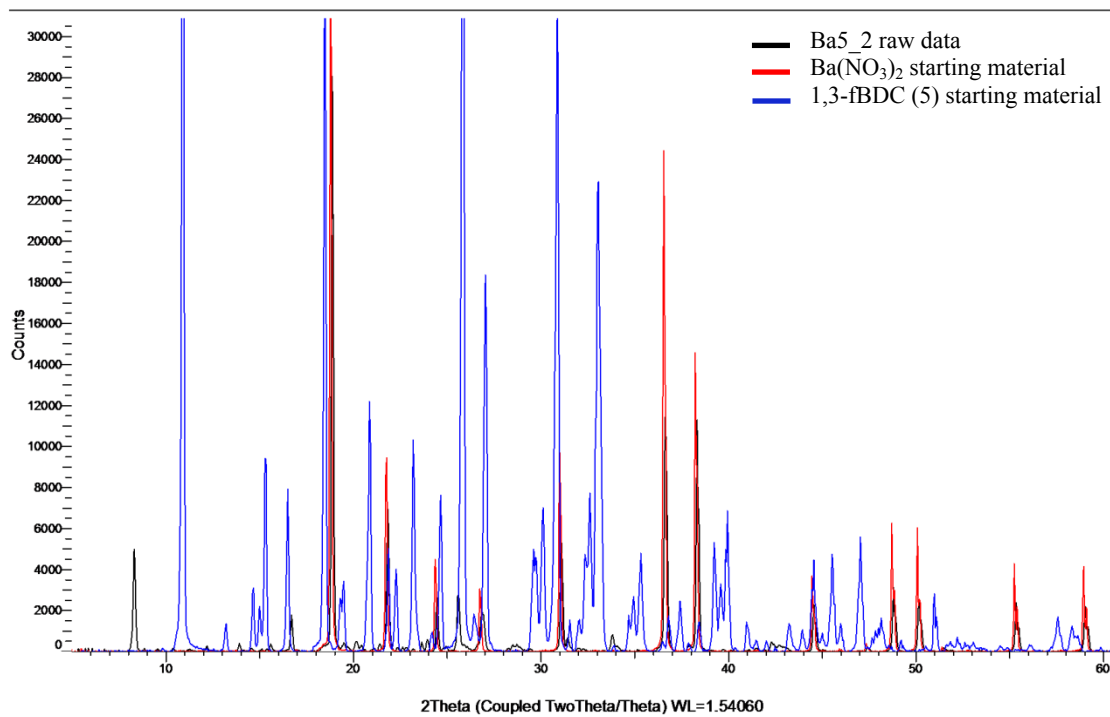


Figure S45 - Ba5_2 Starting Material Overlay

Ca6_1 observed vs. calc.

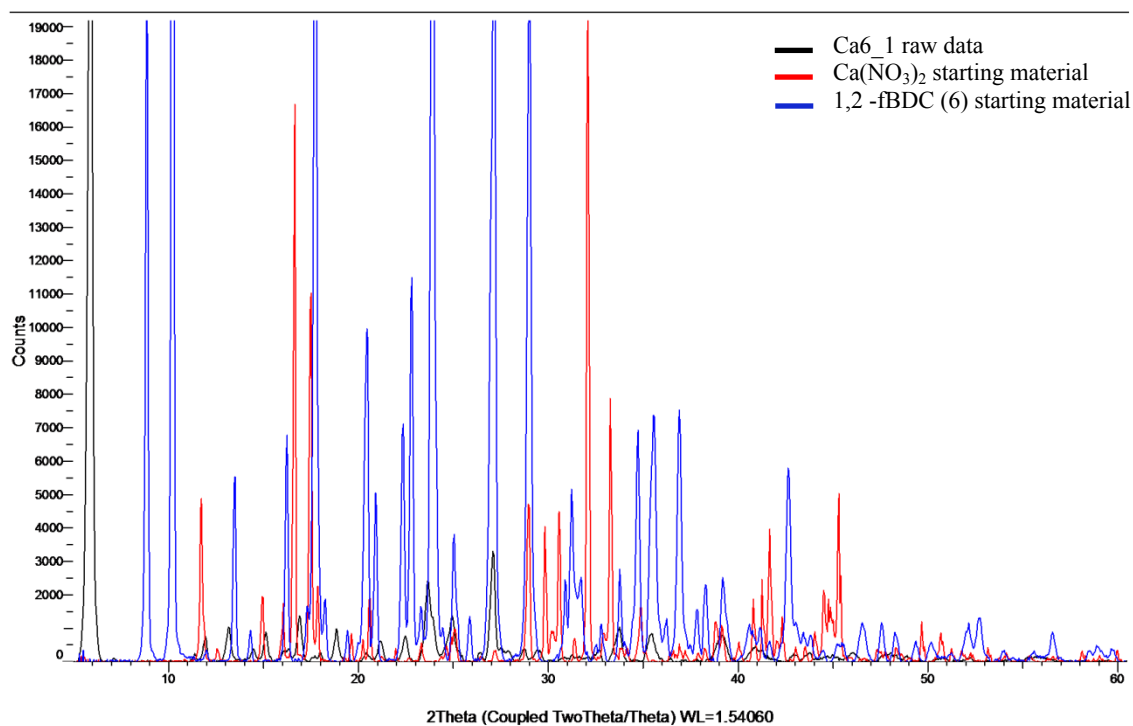


Figure S46 - Ca6_1 Starting Material Overlay

Ba6_1 observed vs. calc.

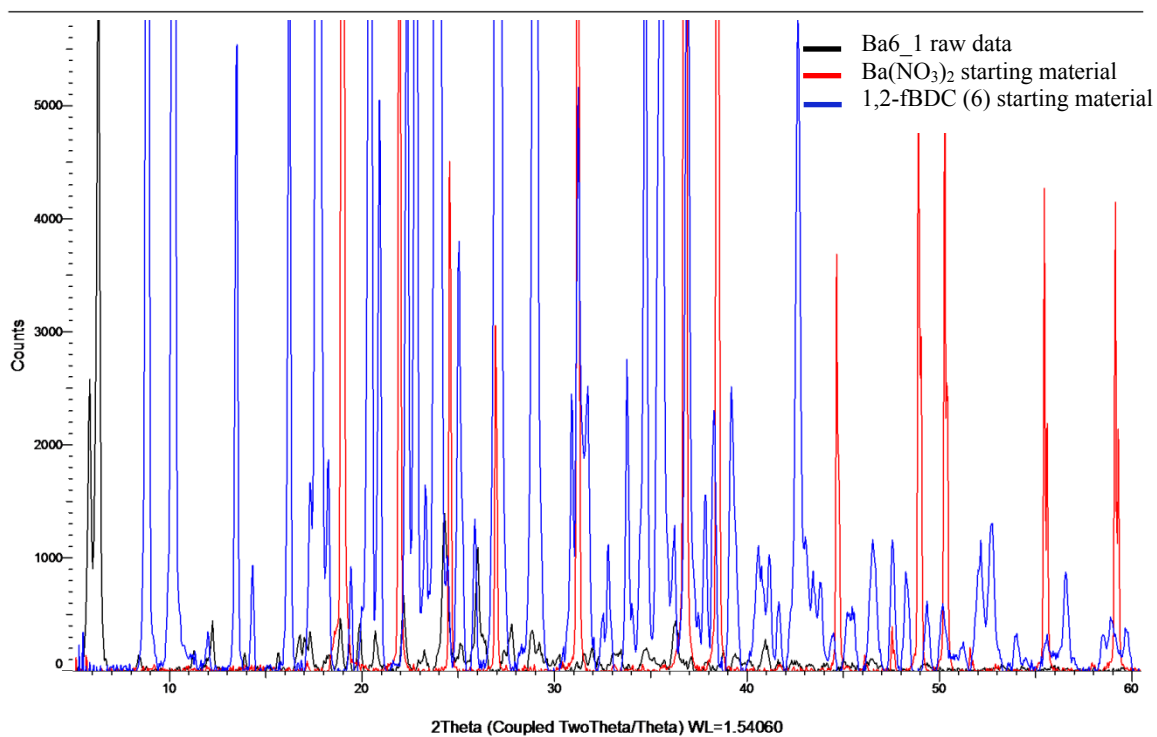


Figure S47 - Ba6_1 Starting Material Overlay

4.4 DSC Traces (under nitrogen)

The thermal analysis of each MOF described below was carried out using a Mettler-Toledo differential scanning calorimeter instrument, model DSC821e, equipped with a liquid nitrogen low temperature attachment and a TSO801RO Universal sample robot (heating rate: $10^{\circ}\text{Cmin}^{-1}$; the flow rate of nitrogen gas: 40ml/min; the sample size: 4 – 10mg in 40 μl aluminium dishes).

The DSC traces below compares the thermal effects of incorporating different metals, Ca(black), Sr(red), and Ba(blue), along with either BDC or fBDC in a MOF using solution method 1 (DMF).

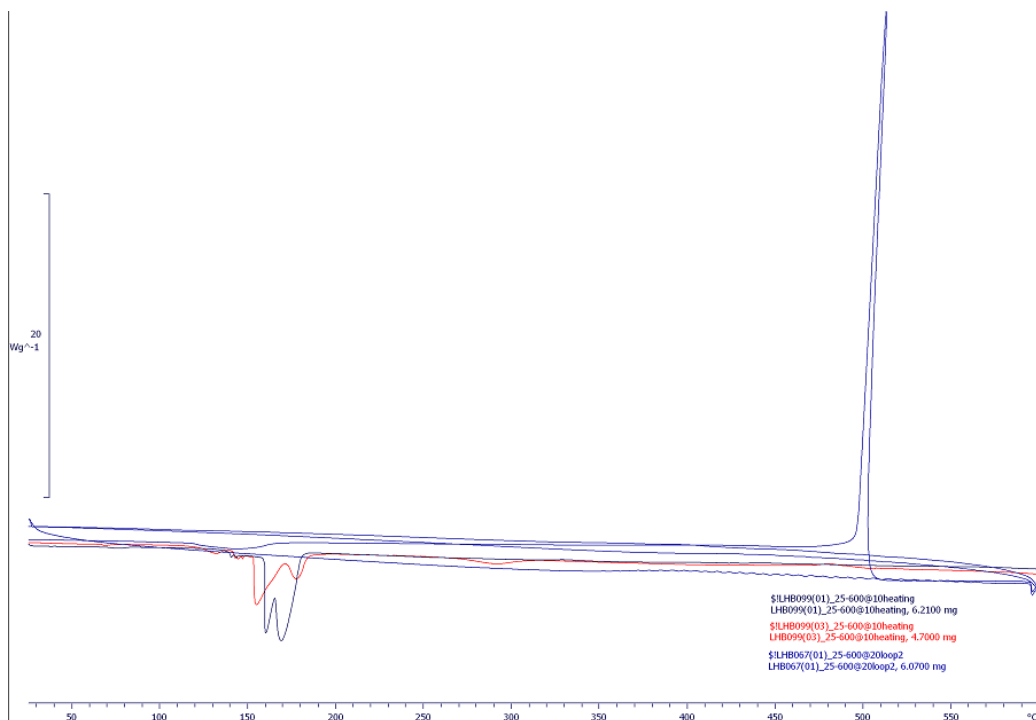


Figure S48 – 1,4-BDC vs Metal DSC Trace

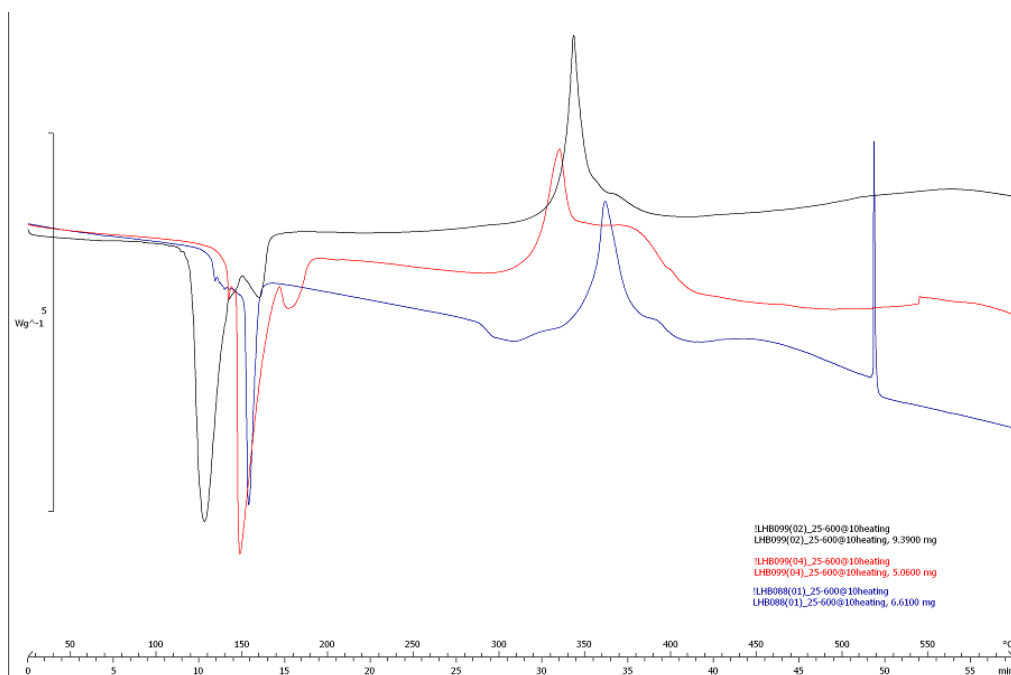


Figure S49 – 1,4-fBDC vs Metal DSC Trace

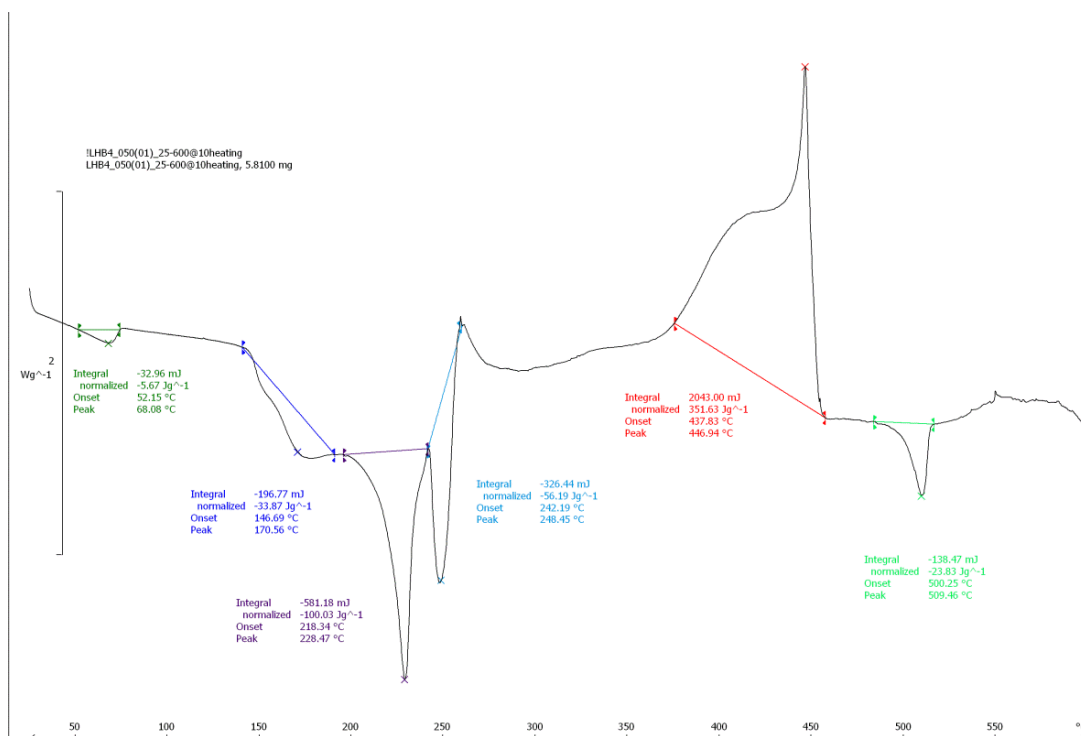


Figure S50 – Ca4_2 DSC Trace

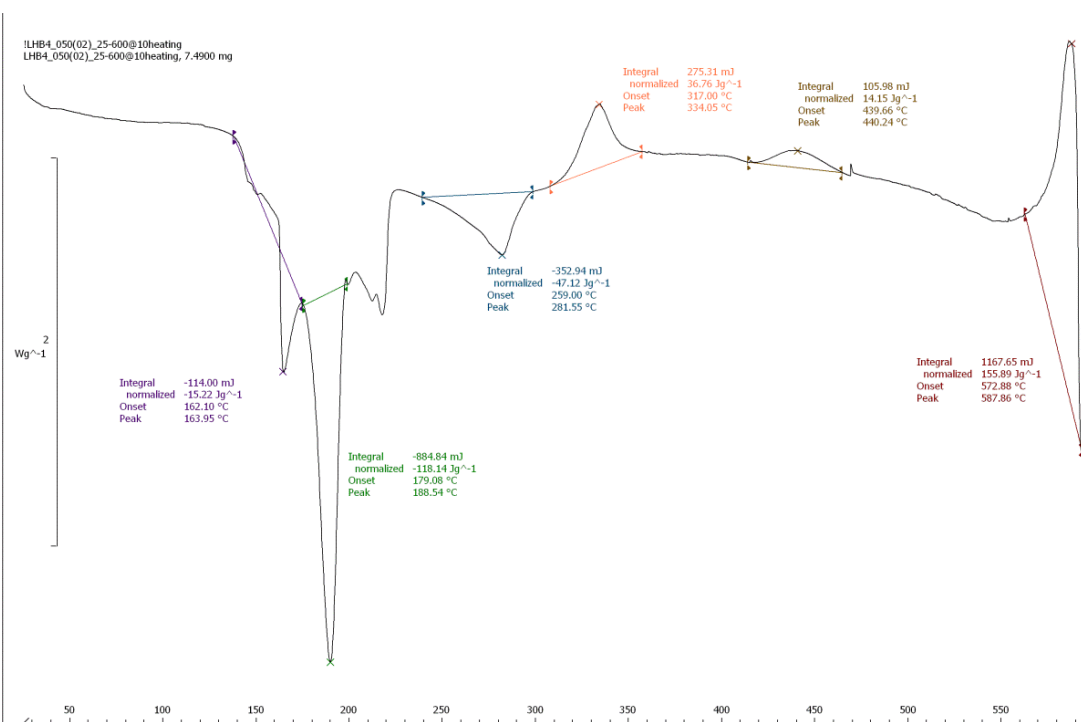


Figure S51 – Sr4_2 DSC Trace

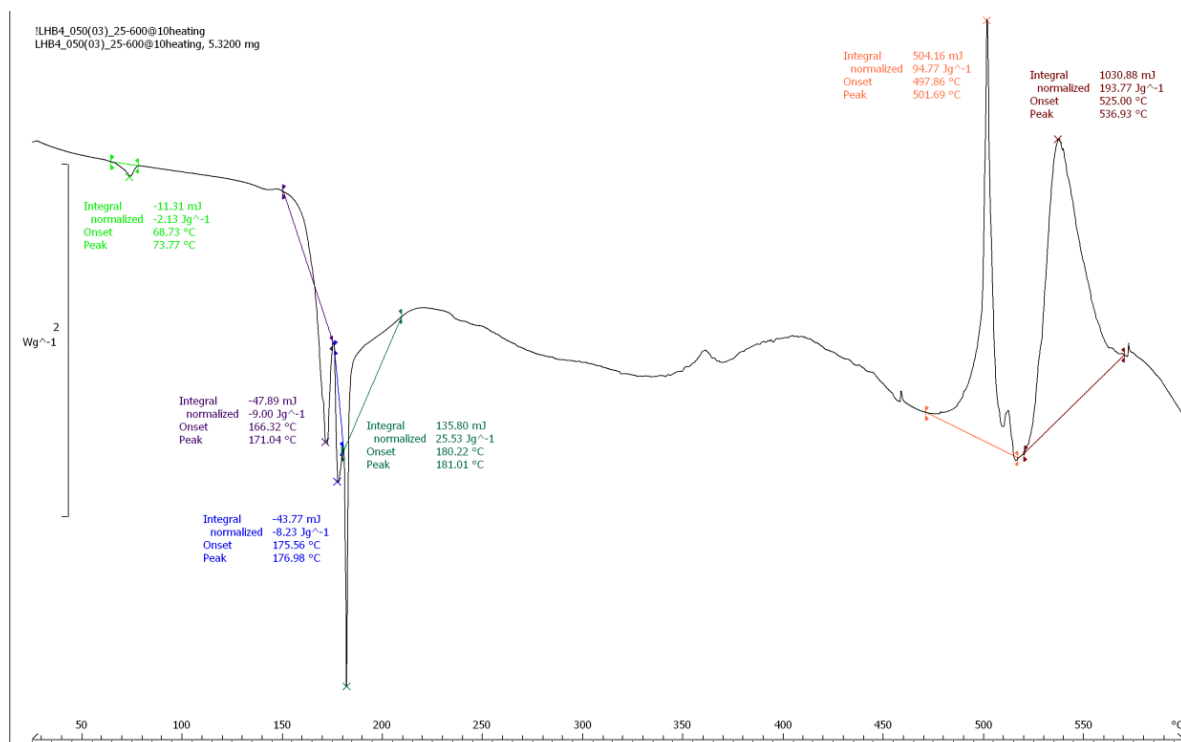


Figure S52 – Ba4_2 DSC Trace

A number of Ba containing products show a peak positioned at the same point (~500°C). A decomposition product expected to result from heating these materials to high temperatures is barium oxide. This reacts at 500–600 °C with air to form barium peroxide, which decomposes at above 700 °C by releasing oxygen.^[10]

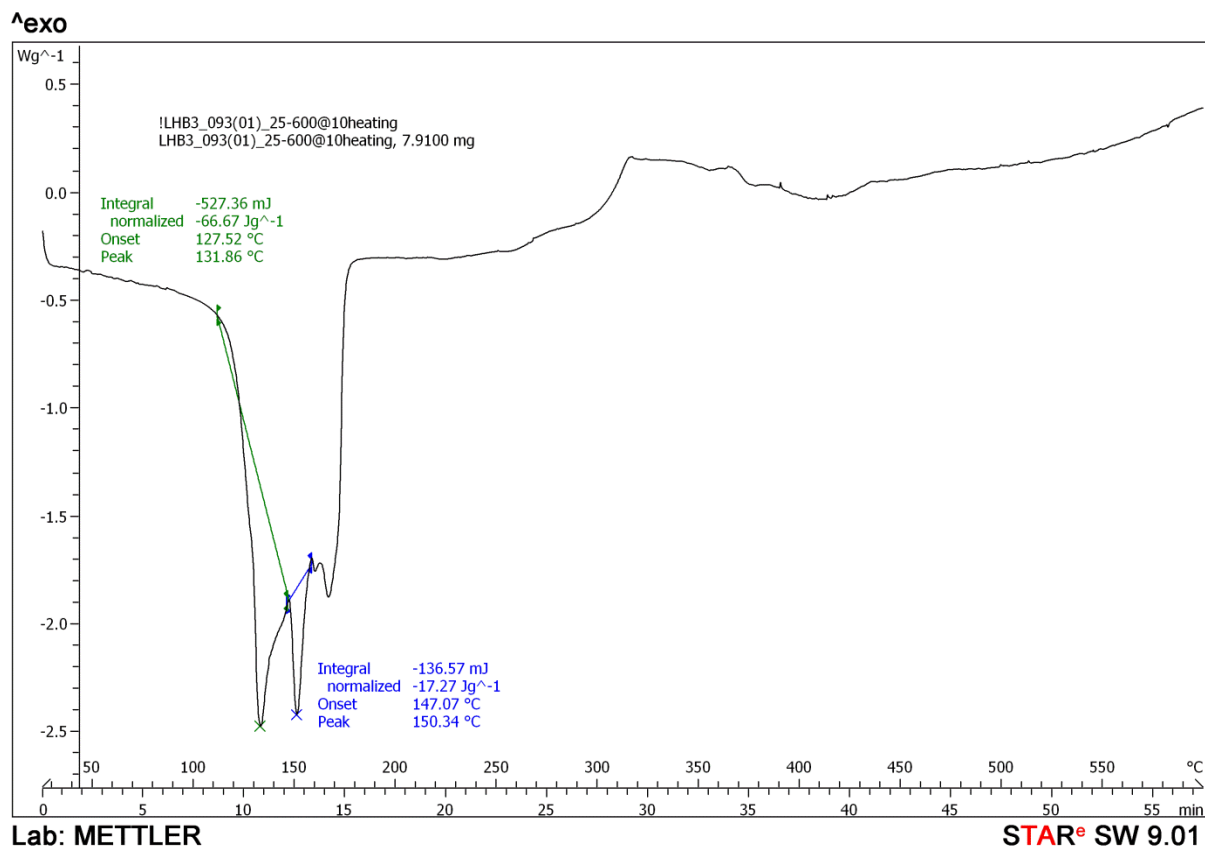


Figure S53 – Ca5_1 DSC Trace

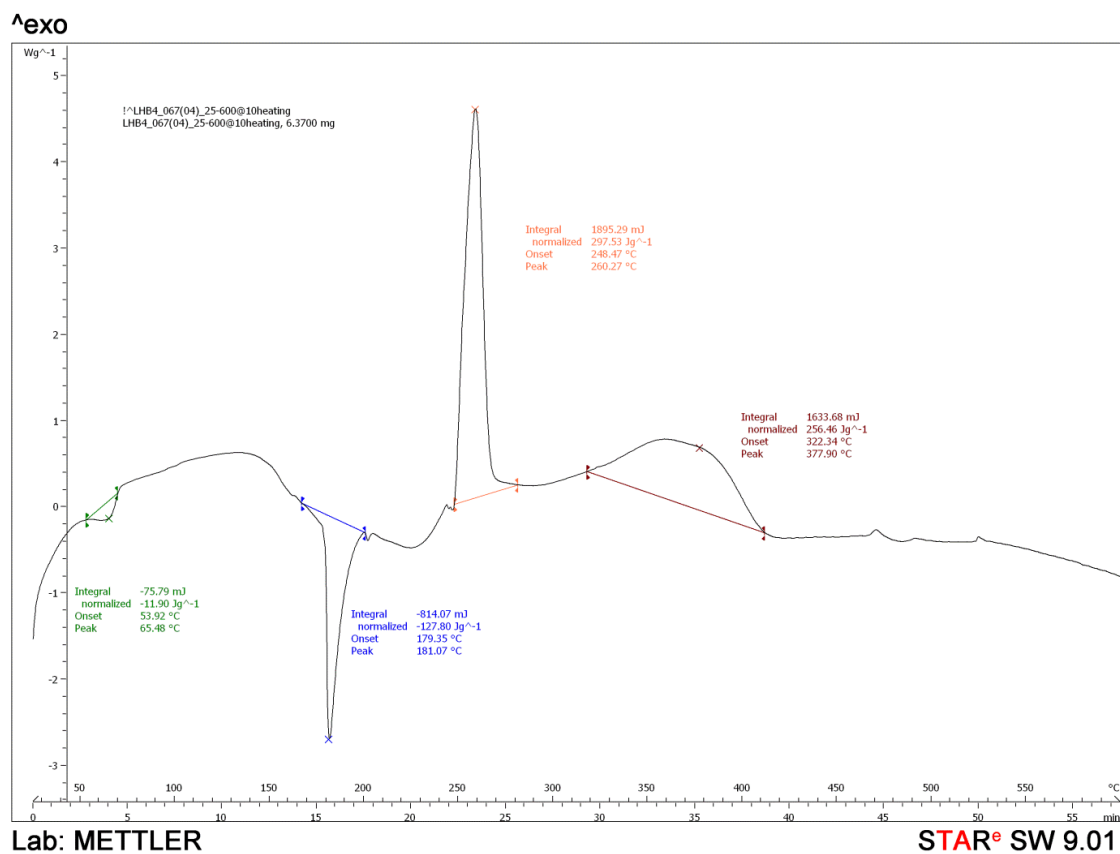


Figure S54 – Ca5_2 DSC Trace

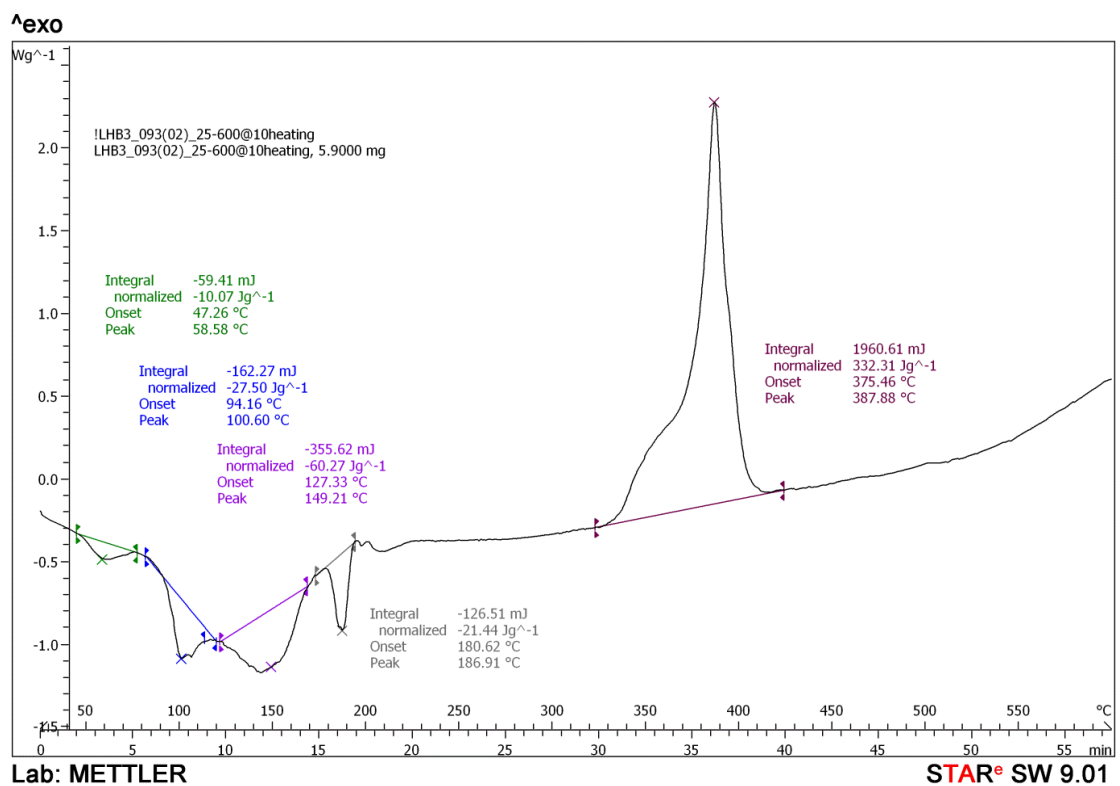


Figure S55 – Sr5_1 DSC Trace

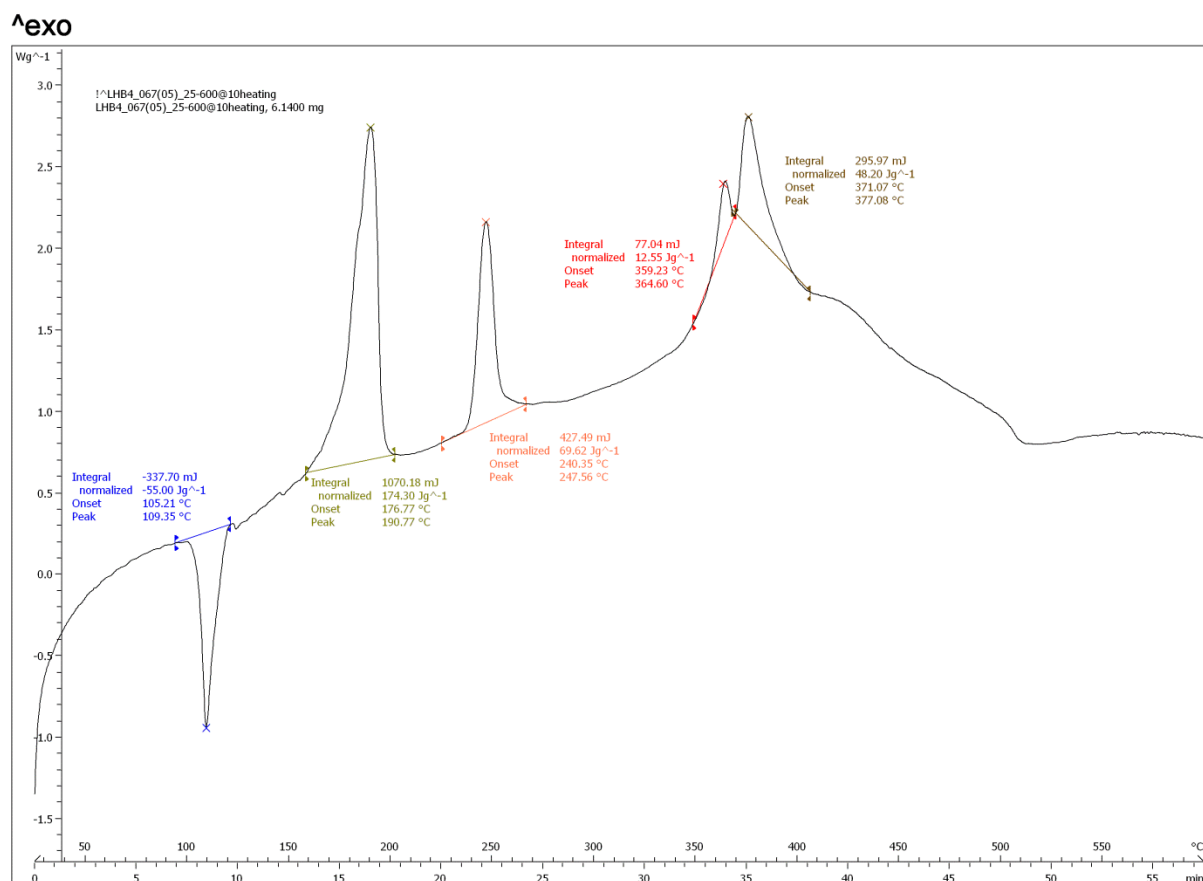


Figure S56 – Sr5_2 DSC Trace

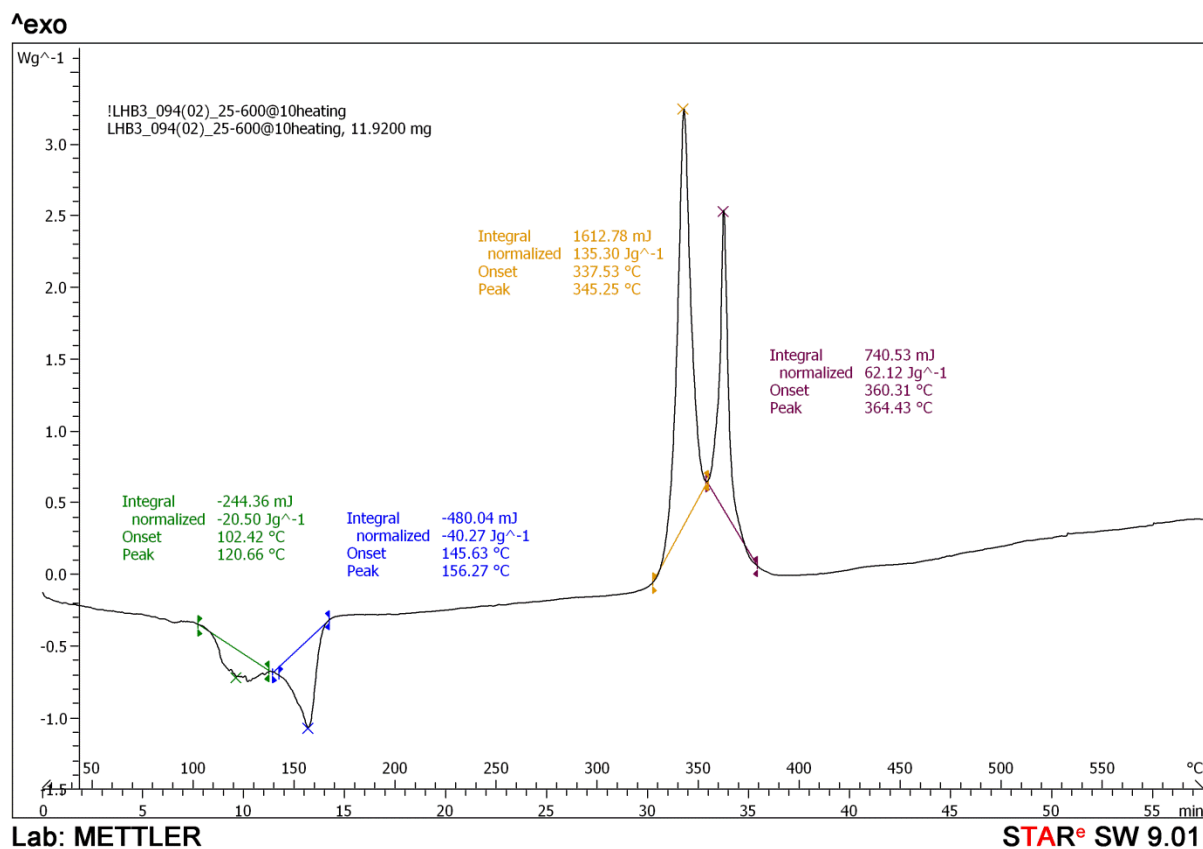
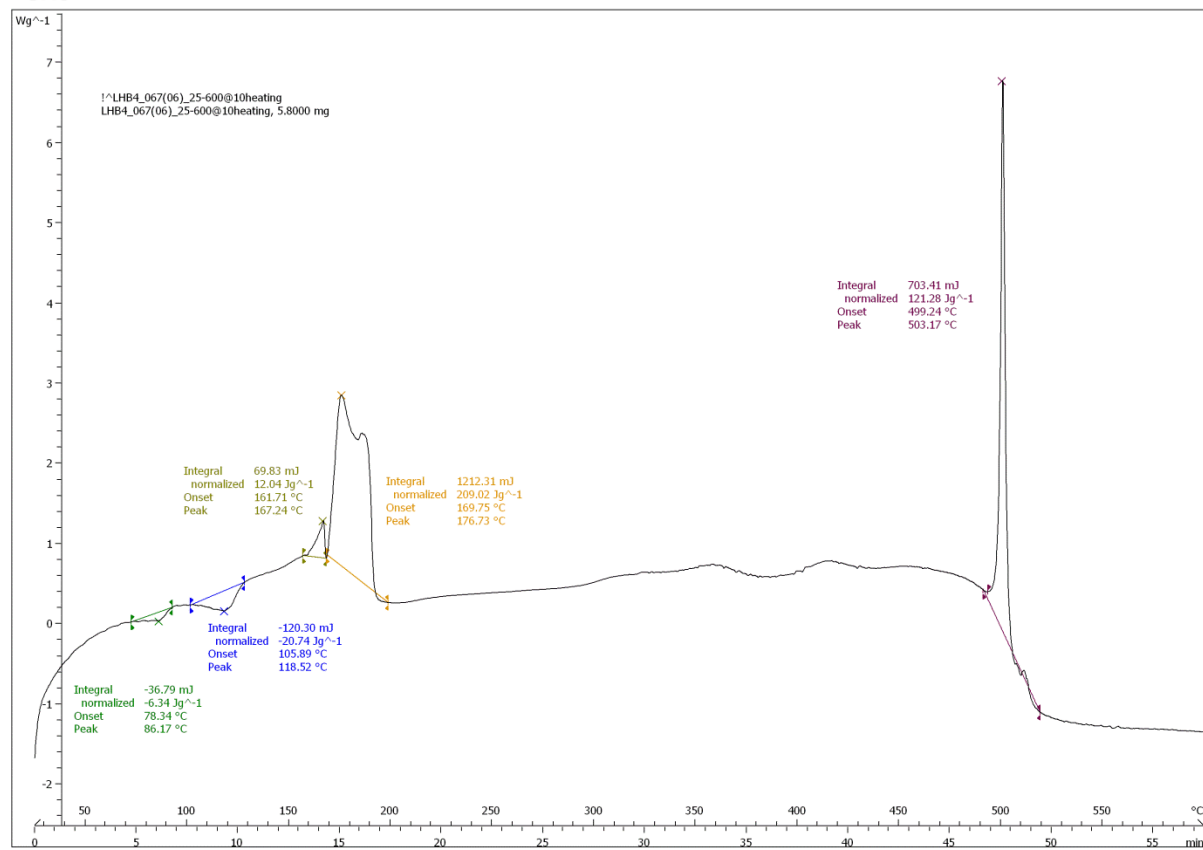


Figure S57 – Ba5_1 DSC Trace

^{exo}

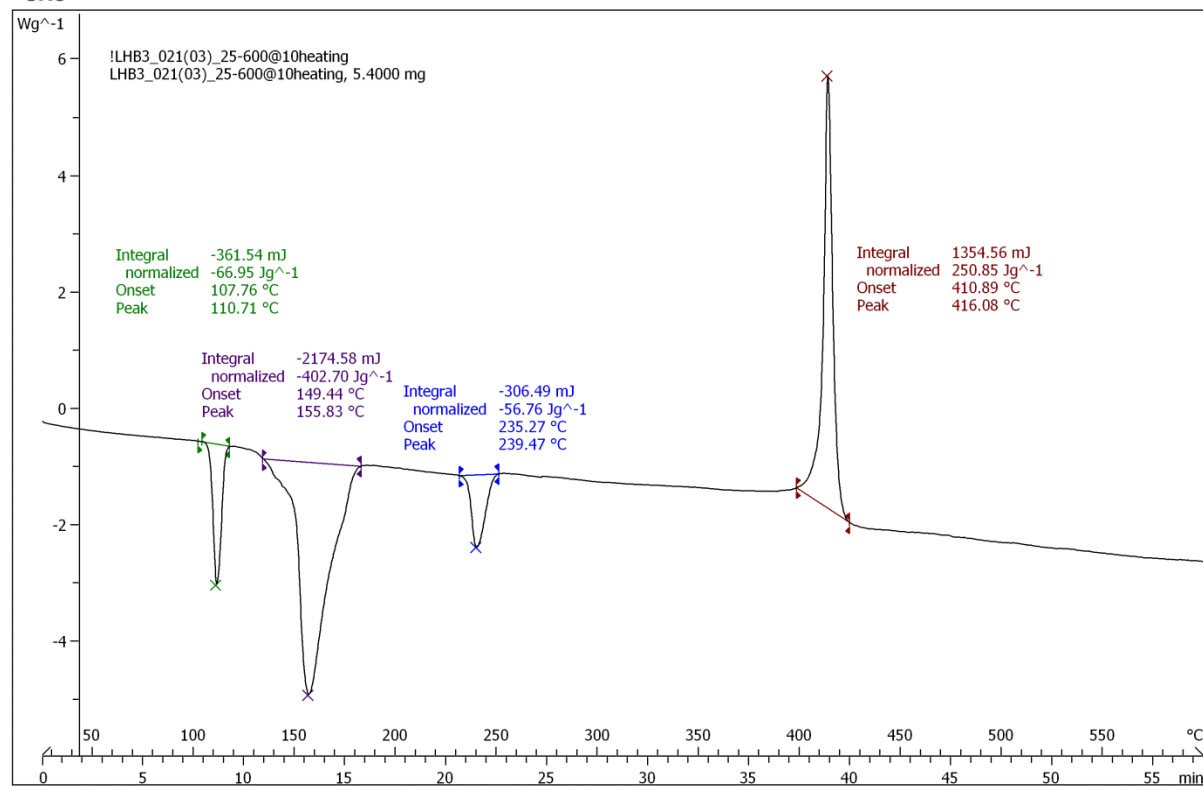


Lab: METTLER

STAR^e SW 9.01

Figure S58 –Ba5_2 DSC Trace

^{exo}



Lab: METTLER

STAR^e SW 9.01

Figure S59 – Ca6_1 DSC Trace

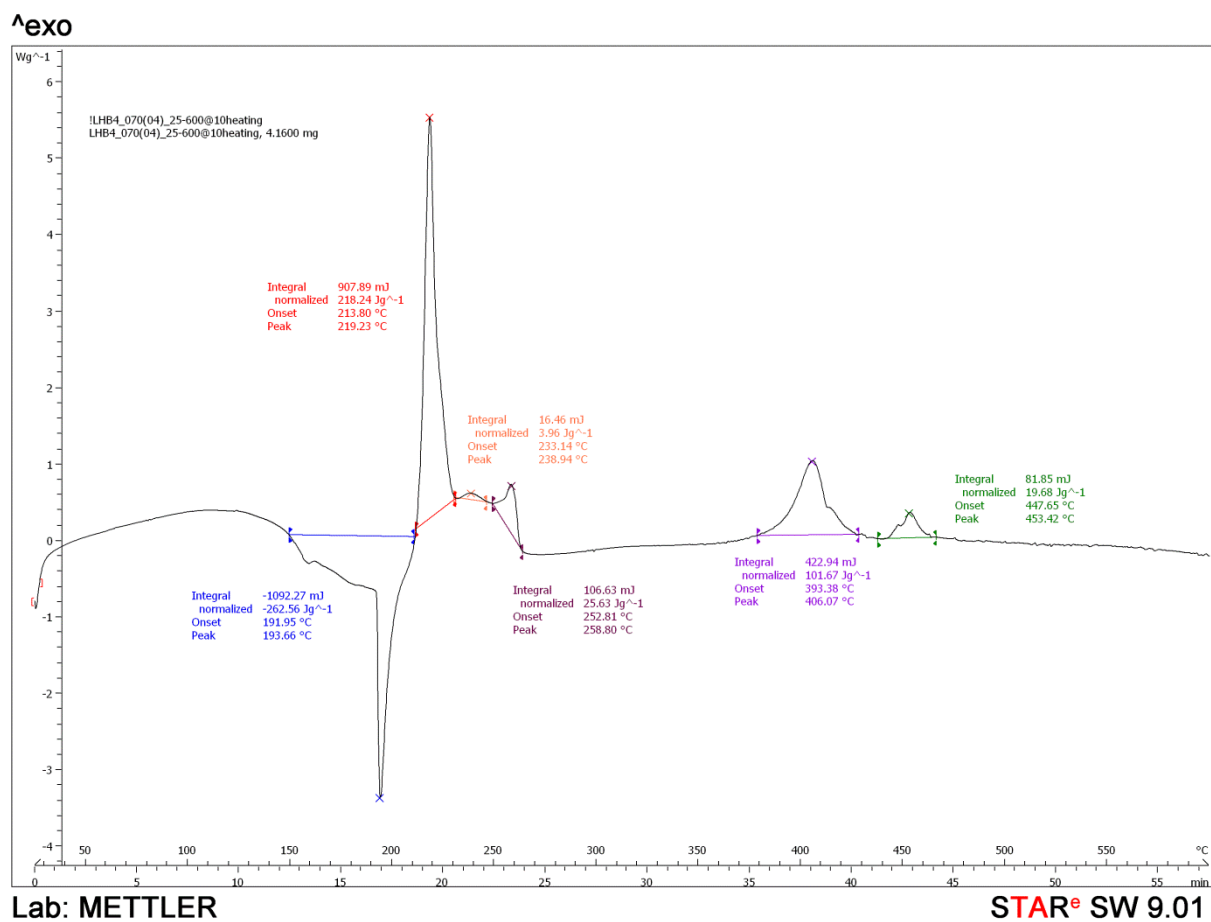


Figure S60 – Ca6_2 DSC Trace

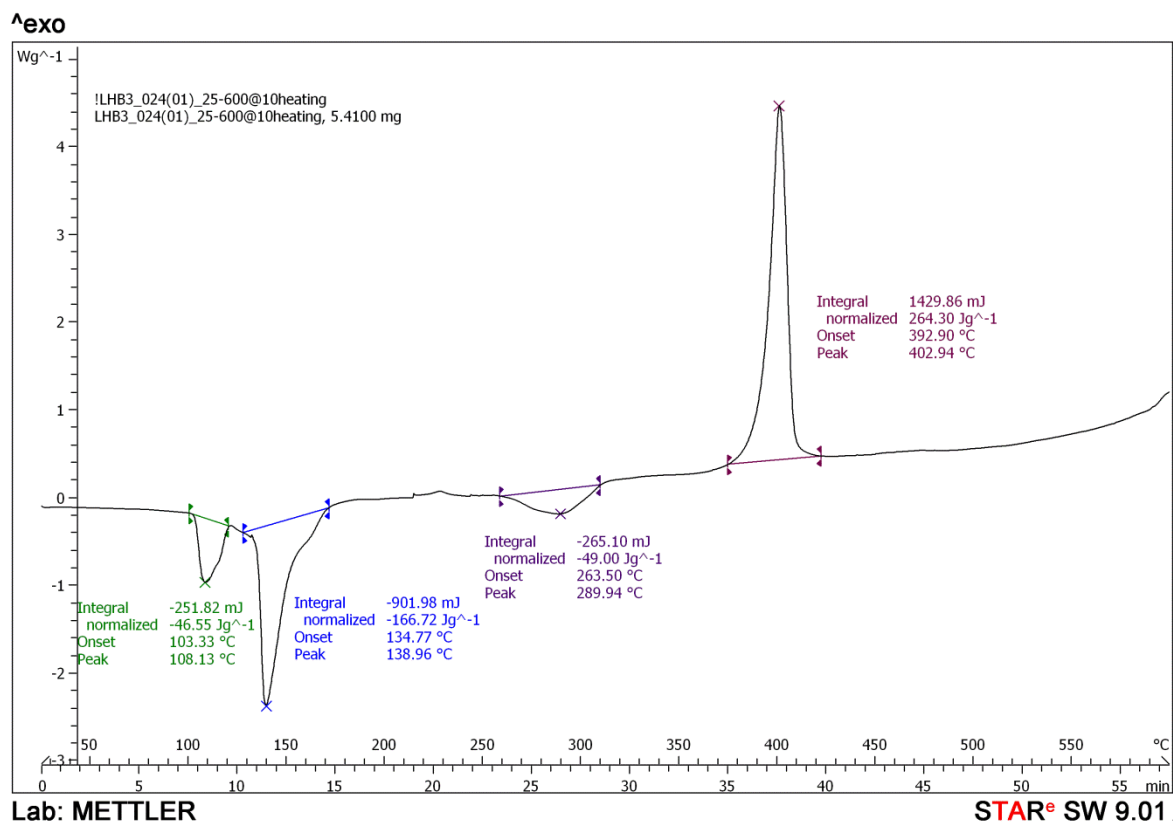
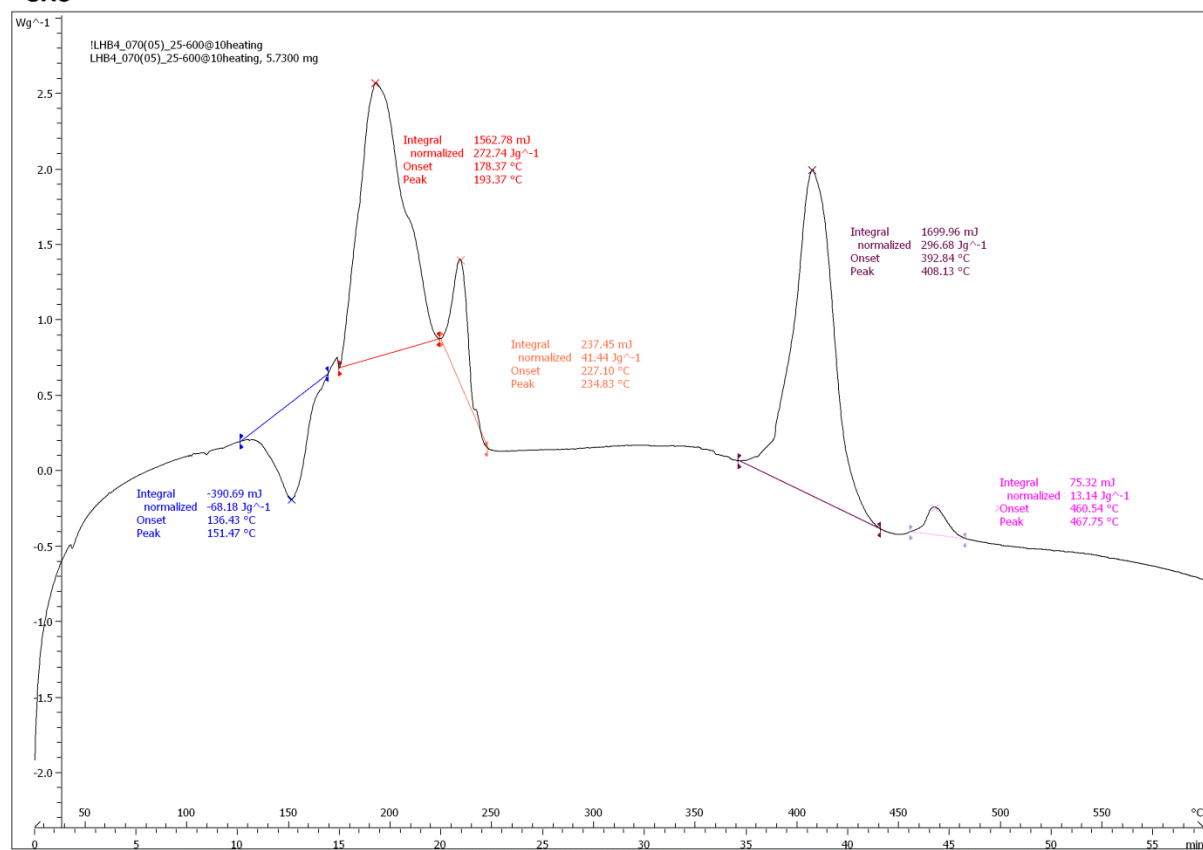


Figure S61 – Sr6_1 DSC Trace

^{exo}

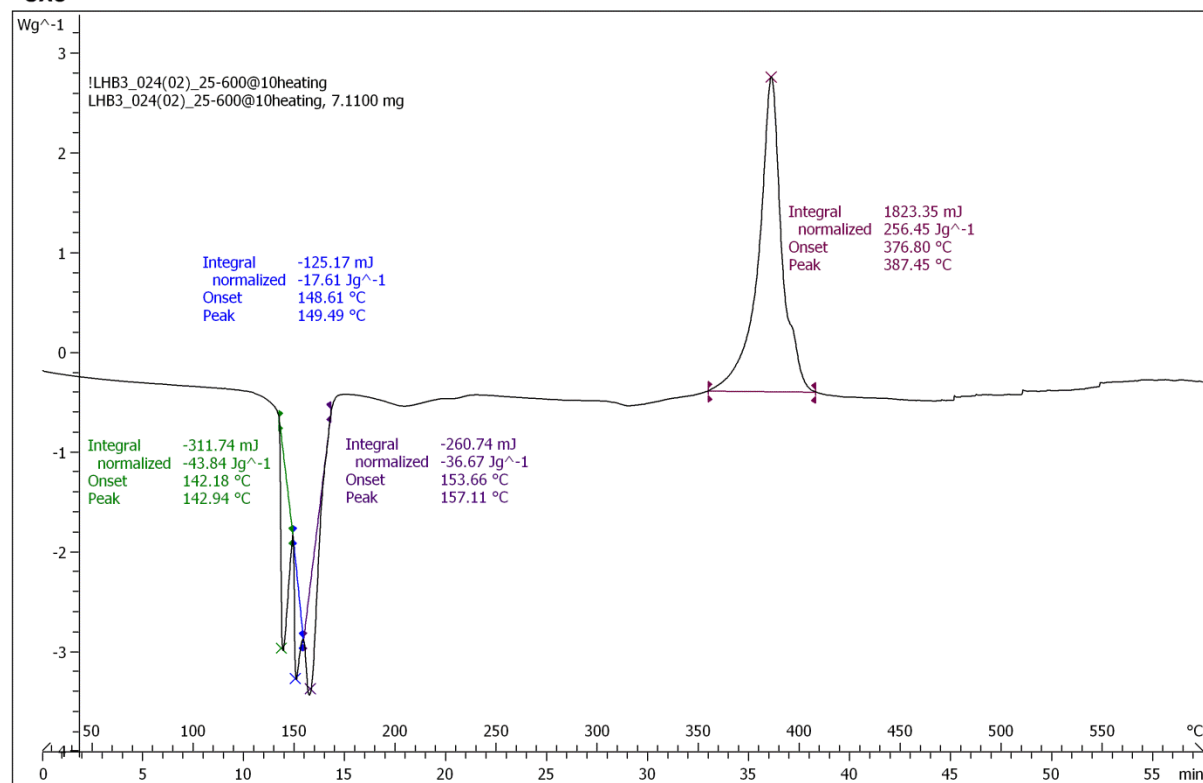


Lab: METTLER

STAR^e SW 9.01

Figure S62 – Sr6_2 DSC Trace

^{exo}



Lab: METTLER

STAR^e SW 9.01

Figure S63 – Ba6_1 DSC Trace

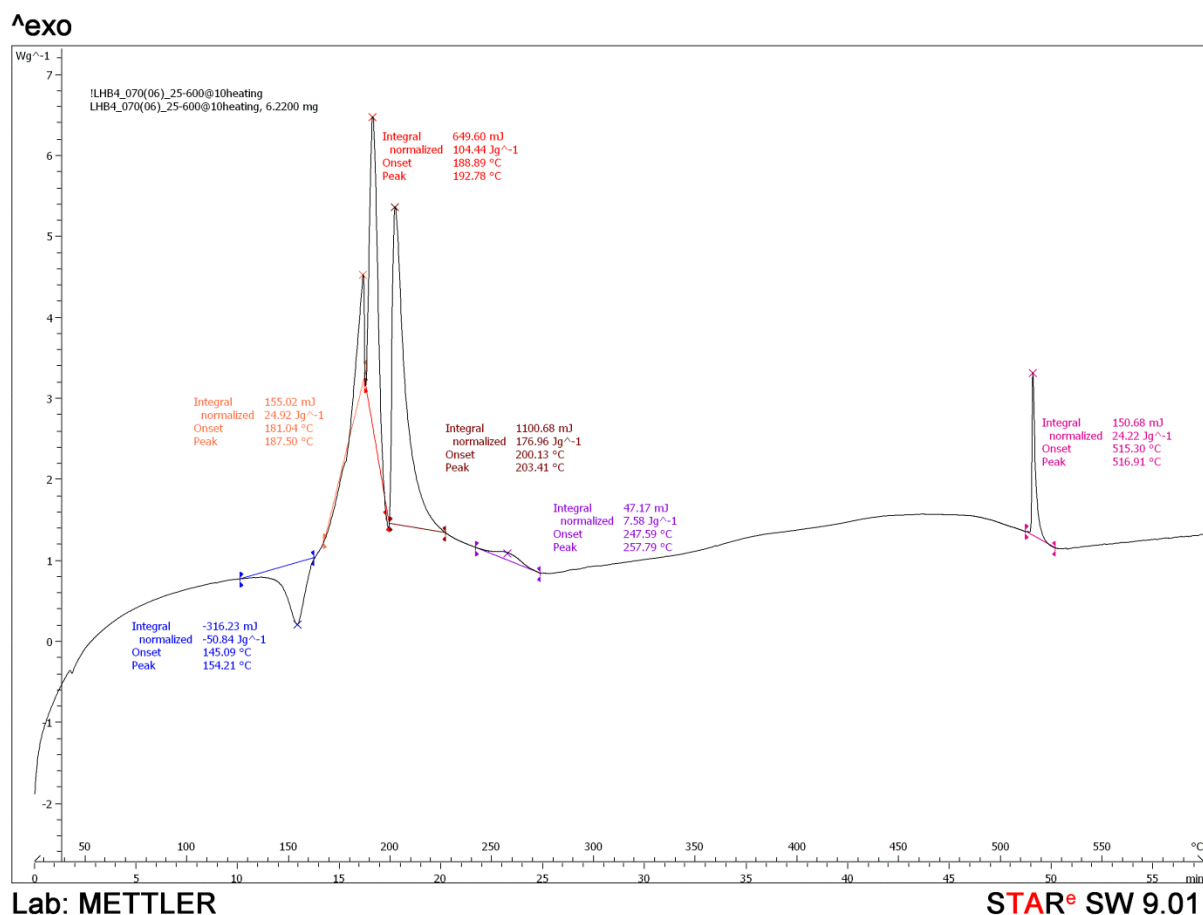


Figure S64 – Ba6_2 DSC Trace

Several of the fluorinated products showed similar thermal decomposition patterns with only Ca5_1 being unique showing no exothermic peaks. Similarities are seen between Sr5_1 and Ba5_1. They show endothermic peaks at around 150°C and then an exothermic peak(s) occurring nearer 350°C. Ca6_1, Sr6_1 also produce a similar pattern; a collection of three or so endothermic peaks followed by a larger exothermic peak. Ba6_1 resembles these patterns also but only loosely. Car5_2, Sr5_2 and Ca6_2 reveal a rapid transition into an exothermic event occurs immediately after an initial endothermic reaction. Sr6_2 and Ba6_2 both produce two exothermic events although the second peak appears much later for the Ba product. These patterns appear to arise as a consequence of the synthetic method used as the similarities only seem to appear when comparing across a series of products resulting from a single approach.

4.5 Burn Tests

The alkaline earth metal MOFs were burn tested within a fume hood on top of a heat proof mat which had a small enclosure mounted on top of it to minimise the effects of the airflow on the burn test. Approximately 15mg of sample was placed into an aluminium DSC lid. The lid was then transferred onto a heat proof tile and ignited using a blow torch. Photographs were taken by Sharif Ahmed using a Canon EOS 7D camera (exposure 1/100 sec).

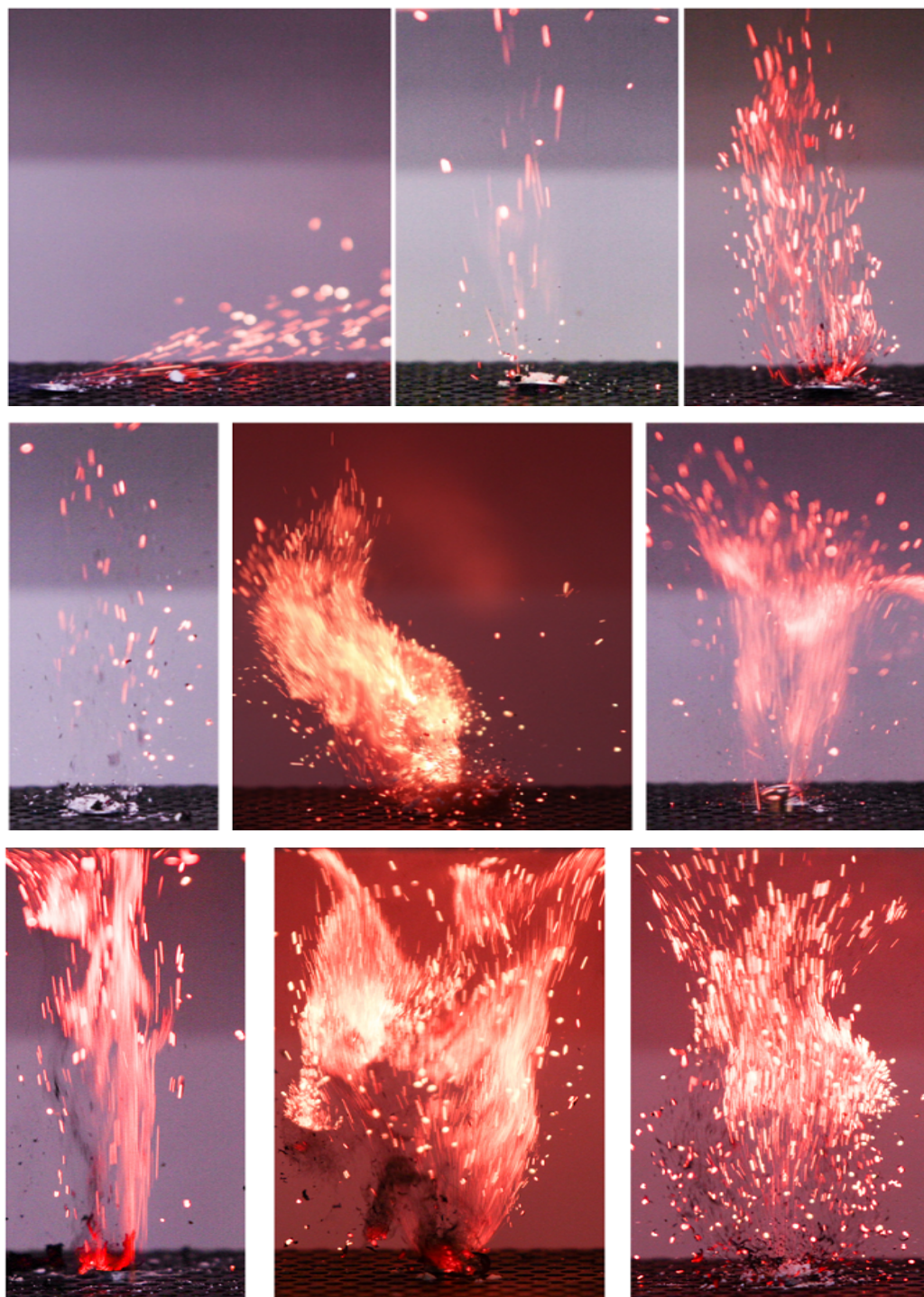


Figure S65 - 1st Route synthesis : (1st row Ca, Sr, Ba 1,4 fBDC, 2nd row Ca, Sr, Ba 1.3-fBDC, 3rd row Ca, Sr, Ba 1,2-fBDC)



Figure S66 - 2nd Route synthesis : (1st row Ca, Sr, Ba 1,4 fBDC, 2nd row Ca, Sr, Ba 1,3-fBDC, 3rd row Ca, Sr, Ba 1,2-fBDC)

References:

- [1] D. Saha, S. Deng, Z. Yang, *J. Porous Mater.* **2009**, *16*, 141-149.
- [2] W. Clegg, L. Russo, *Crystal Growth & Design* **2009**, *9*, 1158-1163.
- [3] M. Werker, B. Dolfus, U. Ruschewitz, *Z. Anorg. Allg. Chem.* **2013**, *639*, 2487-2492.
- [4] A. L. Spek, Utrecht University, Utrecht, The Netherlands., **2002**.
- [5] CrysAlisPro Agilent Technologies, (compiled Aug 13 2014, 1.171.37.35 (release 13-08-2014 CrysAlis171 .NET) ed., **2014**.
- [6] A. Drozdov, A. Pozhitkov, S. Troyanov, A. Pisarevsky, *Polyhedron* **1996**, *15*, 1731-1735.
- [7] aS. H. Dale, M. R. J. Elsegood, *Acta Crystallographica Section E* **2003**, *59*, m586-m587; bH. el Hajjouji, E. Belmonte, J. Garcia-Lopez, I. Fernandez, M. J. Iglesias, L. Roces, S. Garcia-Granda, A. El Laghdach, F. Lopez Ortiz, *Organic & Biomolecular Chemistry* **2012**, *10*, 5647-5658; cB. G. Cooksey, L. T. Gibson, A. R. Kennedy, D. Littlejohn, L. Stewart, N. H. Tennent, *Acta Crystallographica Section C* **1999**, *55*, 324-326; dC. Borel, K. Davies, P. Handa, G. Hedberg, C. L. Oliver, S. A. Bourne, M. Håkansson, V. Langer, L. Öhrström, *Crystal Growth & Design* **2010**, *10*, 1971-1978.
- [8] aP.-Z. Hong, W.-D. Song, Z.-H. Wu, *Acta Crystallographica Section E* **2007**, *63*, m2296; bG. Marinescu, M. Andruh, M. Julve, F. Lloret, R. Llusa, S. Uriel, J. Vaissermann, *Crystal Growth & Design* **2004**, *5*, 261-267.
- [9] in *DIFFRAC.EVA.2.1* (Ed.: B.-A. DIFFRAC.EVA.2.1), Bruker-AXS©, **2010-2012**.
- [10] W. B. Jensen, *J. Chem. Educ.* **2009**, *86*, 1266.